Title
Determining Current Distributions Governed by Laplaces's Equation

Authors
West, A.C.
Newman, J.

Publication Date
1989-11-24

LBL-28075
Preprint

Lawrence Berkeley Laboratory
UNIVERSITY OF CALIFORNIA

Materials & Chemical Sciences Division

To be submitted for publication

Determining Current Distributions Governed by Laplaces's Equation

A.C. West and J. Newman

November 1989

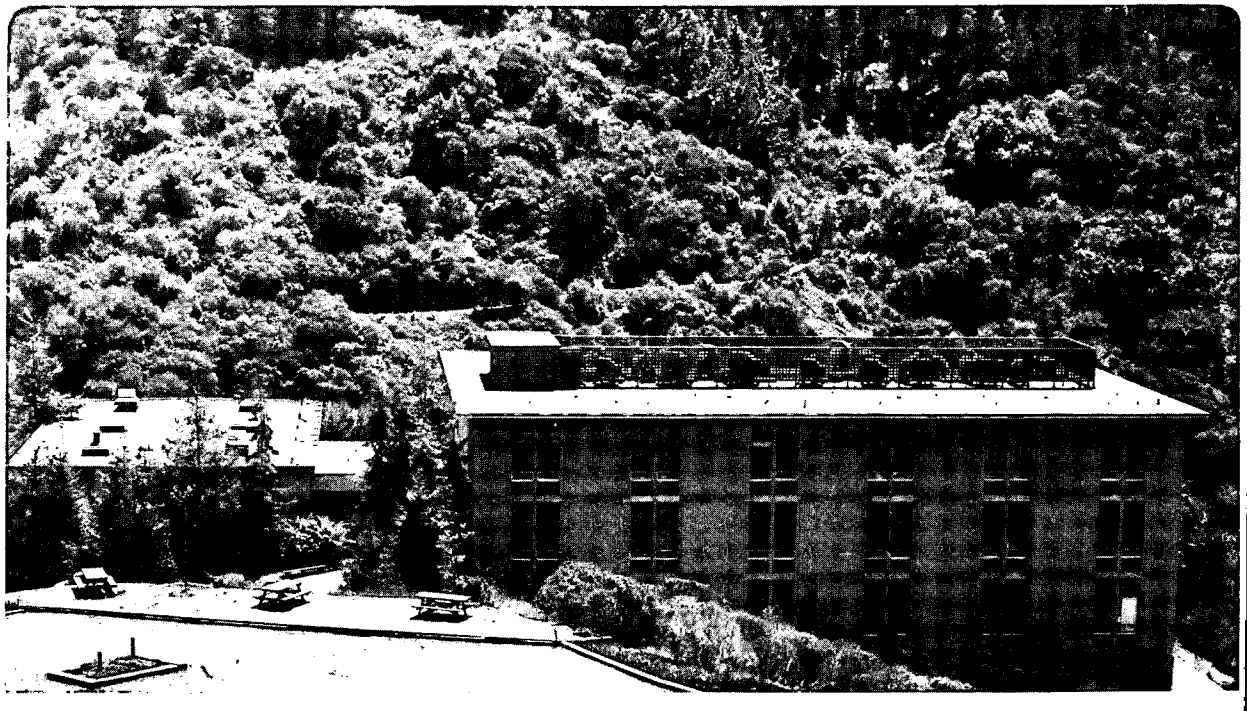

Prepared for the U.S. Department of Energy under Contract Number DE-AC03-76SF00098.

DISCLAIMER

LBL-28075

Determining Current Distributions Governed by Laplace's Equation

Alan C. West and John Newman

Materials and Chemical Sciences Division, Lawrence Berkeley Laboratory,
and Department of Chemical Engineering, University of California,
Berkeley, California 94720

November 24, 1989

1. Introduction

This review summarizes techniques for solving Laplace's equation,

$$\nabla^2\Phi = 0. \tag{1}$$

An emphasis is placed on analytic procedures and how they can be used with numerical methods to obtain accurate solutions at relatively low computer costs. Analytic procedures are also important because asymptotic solutions provide valuable validations of numerical calculations and insights into how results are best displayed and correlated.

By studying in detail the rotating disk electrode [1] (see also [2]), the framework for determining theoretically the current distribution under the condition where both migration and convective mass transfer are important was established. Other important geometries for which this general problem has been investigated include the flow-channel reactor [3], [4], the rotating ring-disk electrode system [5], and the tubular reactor [6].

For the most general current distribution problem, if a mass-transfer boundary layer exists and electroneutrality holds in the bulk solution, Laplace's equation, coupled with other transport equations, must be solved. The discussion will, therefore, remain relevant to these problems, even though the examples are limited to problems where Laplace's equation dictates completely the current distribution. Specifically, the determination of potential and current density distributions in the absence of concentration variations is discussed. Laplace's equation also describes diffusion-limited current distributions when migration, convection, and transients are neglected.

Current distribution problems in which concentration variations are neglected are called *primary* or *secondary*, depending on the boundary conditions specified along the electrode. As a first approximation, concentration variations are negligible when the average current density is much less than the mass-transfer limited, average current density. (If the current distribution is highly nonuniform, the local current density can be so large in certain regions that concentration variations are important, even though the above condition is satisfied.) Since inductance effects are normally only important for times so short as to be of little practical importance, Laplace's equation should also be considered adequate to describe the transient current distribution in response to a step change in the electrode potential, for example.

Recent reviews related to the solution of current distribution problems were given by Prentice and Tobias [7] and Ibl [8]. Newman's review [9] is similar in scope, except that it gives more details related to solution techniques. Our goal is the same as Newman's, except that we focus on Laplace's equation and we emphasize how analytic and numerical procedures are complementary tools. Fleck [10] and Kojima [11] summarized geometries for which the primary current distribution has been determined. We discuss principally problems important to electrochemistry, but it is fruitful to explore other literature where Laplace's equation arises (see, for example, [12]). We loosely refer to potential gradients as current densities. In the absence of concentration variations, they are related through Ohm's law.

2. Boundary Conditions

In modeling, most of the interesting characteristics of an electrochemical system enter through its boundary conditions. Particularly, since Laplace's equation and the insulating boundary conditions are homogeneous and linear, the electrochemical parameters enter the problem statement through the electrode boundary conditions. Polarization parameters, therefore, are discussed in that section.

2.1. Insulators

Insulator boundary conditions are straightforward:

$$\frac{\partial \Phi}{\partial n} = 0, \tag{2}$$

where $\partial/\partial n$ signifies the component of the gradient normal to the insulating surface. Insulator boundary conditions are also used to reflect geometric symmetry. The domain over which the calculations are necessary can then be reduced, thus minimizing possibly the computational effort.

2.2. Electrodes

Electrode boundary conditions are more interesting. Depending on the physics and chemistry of the system, the specified condition differs substantially. In this section, the more common boundary conditions and their physical significance are discussed.

2.2.1. Specified Potential Distribution

The *primary* current distribution is obtained when the potential of the solution adjacent to the electrode is set equal to the electrode potential: $\Phi_o = V$. Problems of this nature, sometimes referred to as

Dirichlet-type problems, have been studied extensively because analytic solution procedures are often successful. Conformal mapping procedures [10], [11] are particularly powerful for solving two-dimensional problems. Conformal mapping techniques, though, are limited in their use because, in general, it is difficult to obtain the proper mapping.

Using separation of variables in a coordinate system appropriate for the geometry, Newman [13] determined analytically the primary current distribution on a disk electrode. Primary current distributions require careful numerical analyses [14], [15] since the current distribution is generally very nonuniform.

Physically, a constant potential boundary condition implies that the surface overpotential is negligible compared to the ohmic potential drop in the solution. We sometimes loosely refer to this as a system with very fast kinetics. For any angle of intersection β between the electrode and insulator that is greater than $\pi/2$ radians (see figure 1), the current density at the electrode edge is infinite. This necessarily causes a large, local surface overpotential, which is inconsistent with the original assumption. The primary current distribution is, therefore, almost never realized physically. It is still important to calculate because it gives the ohmic resistance of the cell and because, in the absence of mass-transfer effects, it gives the maximum variation of current density on the electrode. It also provides an important asymptotic limit that may be approached.

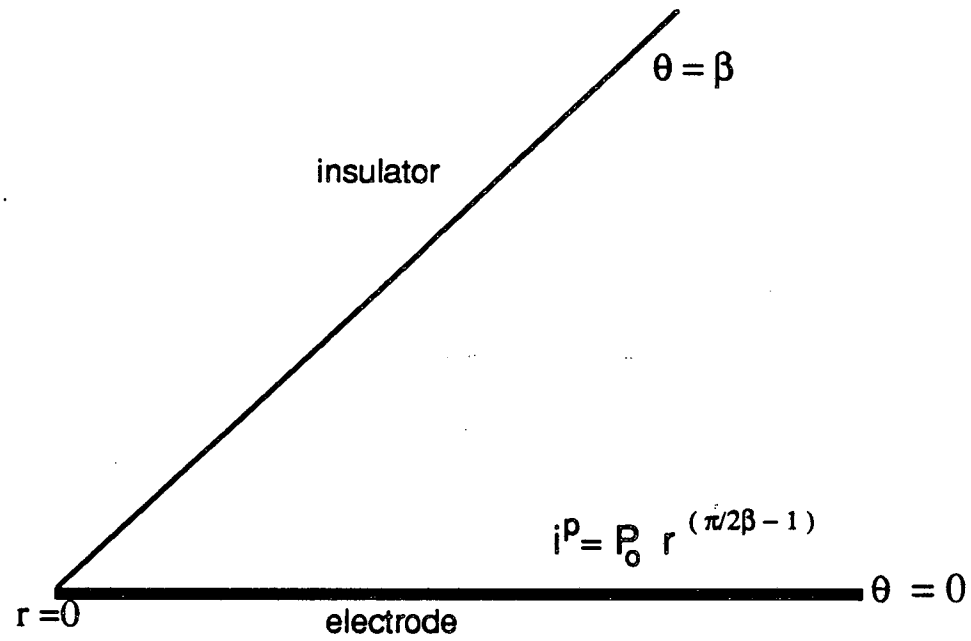

Figure 1. Primary current distribution in the *edge region* of an electrode and insulator.

2.2.2. Specified Current Distribution

A specified constant current distribution is the opposite extreme of a constant potential boundary condition because it corresponds physically to very slow electrode kinetics. Conformal mapping procedures do not handle easily these or other Neumann-type boundary conditions. Historically, these problems, therefore, have not been investigated as extensively as problems with Dirichlet boundary conditions.

Nevertheless, Neumann boundary conditions can be important in electrode design and in the design of corrosion protection systems. For example, White and Newman [16] discussed the effect that side reactions have on the shape of limiting current curves obtained on a rotating disk electrode. They discussed the importance of calculating the maximum variation in the solution potential adjacent to the working electrode. For the disk electrode, the maximum difference in potential between the center and edge occurs for a constant current distribution [2], [17]:

$$(\Delta\Phi_o)_{max} = \frac{0.363 r_o i_{avg}}{\kappa}. \tag{3}$$

A hemispherical pit, investigated in reference [18], represents another geometry of importance in understanding corroding systems.

For some applications, a nonuniform current distribution is specified. For the rotating hemisphere electrode, the mass-transfer-limited current distribution is nonuniform [19]. The corresponding potential distribution on the hemisphere is given in reference [20]. Newman [21], [22] discussed the importance of Neumann boundary conditions in the analysis of corrosion systems. For example, a specified current distribution for the anodic reaction may be dictated by the limiting current

distribution for the reduction of O_2.

2.2.3. Butler-Volmer Equation

More general to a prescribed potential or current distribution is a condition relating the local current density to the local surface overpotential, η_s, which is the potential difference between the electrode and the solution adjacent to the electrode: $\eta_s = V - \Phi_o$. When such boundary conditions are used, the current distribution is called *secondary*. Many electrochemical reactions are described adequately by the Butler-Volmer equation:

$$i = i_o\left[\exp\left[\frac{\alpha_a F\eta_s}{RT}\right] - \exp\left[\frac{-\alpha_c F\eta_s}{RT}\right]\right]. \qquad (4)$$

The nonlinearity of this equation makes it difficult to obtain analytic solutions. This boundary condition, however, is handled easily with numerical techniques. Only for a limited range of intermediate η_s is the full Butler-Volmer equation necessary. Therefore, for many studies, it is desirable to study two simplified forms of this relation because the compilation of results is more straightforward.

Linear Kinetics—For small surface overpotentials, which occur when the average current density is much smaller than the exchange current density, the Butler-Volmer equation is linearized to give the important simplification of linear kinetics,

$$i = \frac{(\alpha_a+\alpha_c)Fi_o}{RT}\,\eta_s. \qquad (5)$$

Since equation (4) can be expressed as

$$i = i_o\left[1 + \frac{\alpha_a F\eta_s}{RT} + \frac{1}{2!}\left(\frac{\alpha_a F\eta_s}{RT}\right)^2 + \cdots\right] \tag{6}$$

$$- i_o\left[1 - \frac{\alpha_c F\eta_s}{RT} + \frac{1}{2!}\left(\frac{-\alpha_c F\eta_s}{RT}\right)^2 + \cdots\right],$$

the linear kinetics approximation applies when $F\eta_s/RT \ll 1$.

Wagner [23] emphasized that equation (4) can also be linearized around a nonzero surface overpotential if its variation is sufficiently small. This procedure is particularly relevant for electroplating where the process is designed to give a relatively uniform current distribution. It is sometimes suggested that the Tafel relationship can always be linearized around some average surface overpotential, and, hence, it is only necessary to solve the linear kinetics case. Wagner [23] stated that this is often an incorrect assertion because the surface overpotential can vary sufficiently that linearization is not valid. Appendix B of West *et al.* [24] shows explicitly by a regular-perturbation analysis when the Tafel kinetics relation, discussed below, is approximated adequately by a linear kinetics relation for the rotating disk electrode.

Tafel Kinetics—A second important simplification of the Butler-Volmer equation occurs at large η_s. For large, anodic surface overpotentials, equation (4) becomes

$$i = i_o \exp\left(\frac{\alpha_a F\eta_s}{RT}\right). \tag{7}$$

This is known as the Tafel kinetics relation and becomes valid when $|i_{avg}| \gg i_o$, that is, when $F\eta_s/RT \gg 1$. An analogous relation can be written for cathodic reactions, where large, negative surface overpotentials may arise.

2.2.4. Polarization Parameters

It is useful to quantify our references to "fast" and "slow" kinetics. In 1940, Kasper [25] discussed the effect of the electrode size on the uniformity of the current distribution. Hoar and Agar [26] discussed more generally, and Wagner [23] subsequently clarified, the importance of the dimensionless group that is now known as the Wagner number:

$$Wa = \frac{\kappa}{L}\left(\frac{d\eta_s}{di}\right)_{i=i_{avg}}, \tag{8}$$

where L is some length characteristic of the electrode geometry. The Wagner number represents the ratio of kinetic to ohmic resistances. The primary current distribution applies when $Wa = 0$, and a constant current density boundary condition is appropriate when $Wa \longrightarrow \infty$. To characterize the current distribution, it is not sufficient to know only the value of the Wagner number since the distribution can differ depending, for example, on whether linear or Tafel kinetics applies.

In this review, we follow Newman [1] in using polarization parameters that are inversely related to the Wagner number. For linear kinetics, the ratio of the ohmic resistance to the kinetic resistance is given by a dimensionless exchange current density:

$$J = \frac{(\alpha_a+\alpha_c)FLi_o}{RT\kappa}. \tag{9}$$

For Tafel kinetics, the exchange current density affects the value of the average surface overpotential but does not influence the distribution of current density. Instead, a dimensionless average current density is the important parameter:

$$\delta = \frac{\alpha_a F L |i_{avg}|}{RT\kappa}. \tag{10}$$

For linear or Tafel kinetics, when there exists one characteristic length, knowledge of the value of J or δ is sufficient to describe the current distribution. J or δ is sufficient to describe completely the current distribution. If the full Butler-Volmer equation is used, it is necessary to specify J, δ, and the ratio of transfer coefficients, α_a/α_c.

It should be remembered that counterelectrodes exist. The current distribution on the counterelectrode influences the current distribution on the working electrode, and the effect increases the closer they are placed together. The effect of bringing the counterelectrode close to the working electrode is readily seen for the primary current distribution in the channel geometry [27]. For a given ratio of the characteristic lengths, West and Newman [28] showed the influence of the counterelectrode polarization parameter on the current distribution on the working electrode.

2.2.5. Passivation Kinetics

The previous two sections focus on equations that can be obtained from a Butler-Volmer equation. Not all electrochemical reactions can be described by such a relationship. Most obviously, passivating systems, where the current density abruptly drops to a small current density at the Flade potential, can not be described by a Butler-Volmer equation.

Because of the experimental difficulties in subtracting the ohmic drop near the active-passive transition, controversy concerning the correct form of the polarization curve exists. Figure 2, taken from

reference [29], shows three possible shapes for the active-passive transition of iron in sulfuric acid. Attention should be focused to the right of the limiting current plateau (near the passivation potential) because the plateau itself is caused by concentration variations, which we are not discussing. Mass-transfer effects principally change the surface pH, which changes the value of the Flade potential [30] but probably has little influence on the shape of the transition.

For simplicity, Law and Newman [31] and Russell and Newman [32] used curve b to try to understand the passivation phenomena observed on the rotating disk electrode. Haili [33] and Newman [21] reviewed the controversy over which of the four curves in figure 2 is the best description. Dukovic [34] also reviewed work concerned with the proper shape of the polarization curve. He presented results related to the anodic protection of 316 stainless steel in 67 percent sulfuric acid. He used an experimental curve that shows an active-passive transition similar to curve b and also includes transpassive dissolution.

For many applications, the precise form of the active-passive transition is not crucial. For simplicity then, it may be easiest to assume a sharp transition.

2.2.6. Transients

When the electrode potential or current is varied with time, it may be necessary to include double-layer charging:

$$i = C \frac{\partial \eta_s}{\partial t} + f(\eta_s). \tag{11}$$

C is the double-layer capacity, and $f(\eta_s)$ relates the faradaic current to the surface overpotential. It may, for example, be a Butler-Volmer

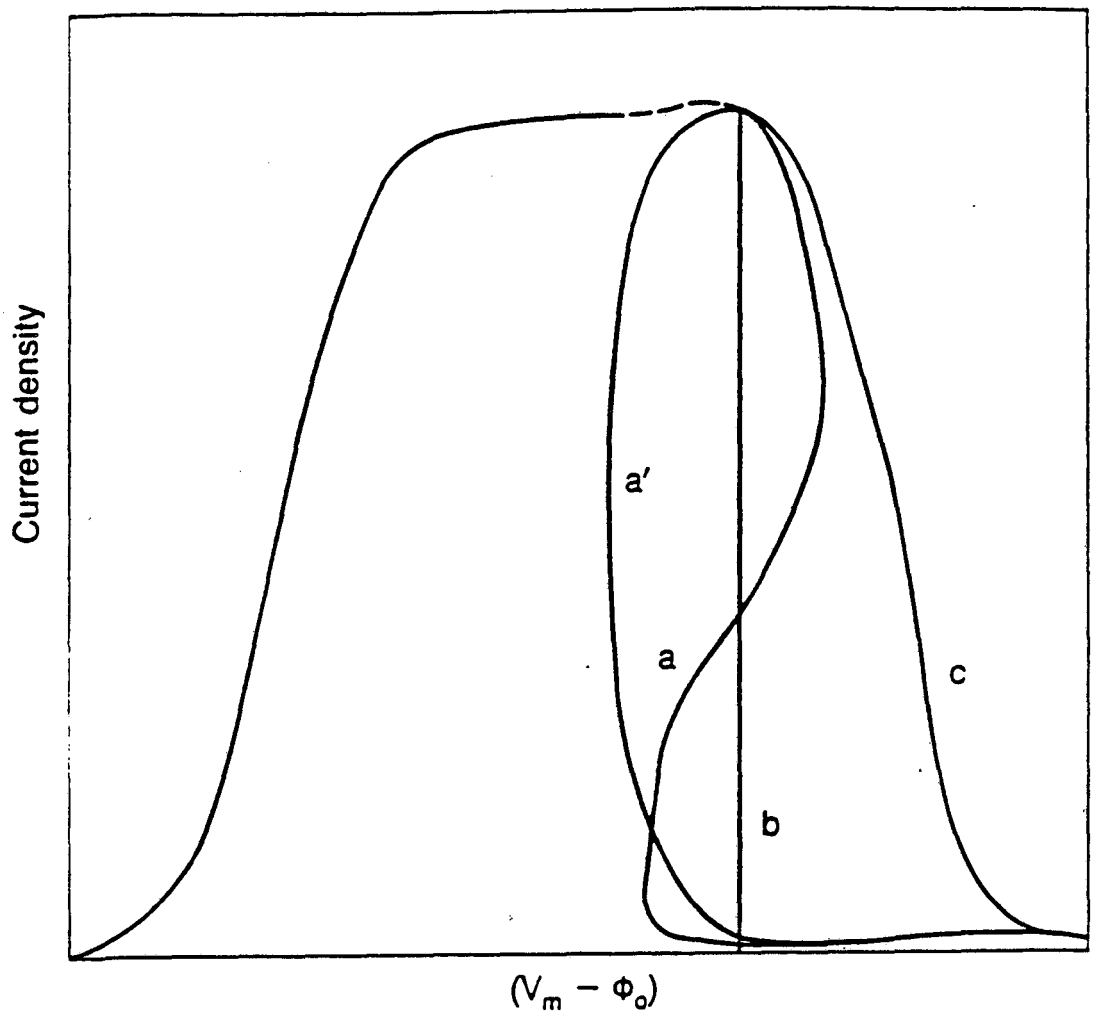

Figure 2. A schematic of the polarization curve for the dissolution of iron in 1 M sulfuric acid, showing four possible paths for the active-passive transition. The figure is taken from reference [29].

relation.

Nişancioğlu and Newman [35], [36], [37] presented a series of papers that describe the transient current distribution on a disk electrode. If the faradaic reaction is described by linear kinetics, the faradaic current is negligible compared to the capacitive current for times $t \ll RTC/Fi_o$. A double layer can be nonuniformly charged. The time that it takes for the charge on an ideally polarizable electrode to redistribute to a uniform state is another characteristic quantity that appears in transient problems. For the rotating disk electrode, this time constant is given by $\tau = r_o C/\kappa$ [38].

Equation (11) suggests that, for a short time after a step change in the current or electrode potential, the primary current distribution is approached. This is well known in the AC impedance literature, where the ohmic resistance is obtained when the frequency $\omega \longrightarrow \infty$ (*i.e.*, $t \longrightarrow 0$). That the current distribution can change with frequency contributes to the phenomenon of frequency dispersion on an electrode with a nonuniform current distribution [39].

2.2.7. Moving Boundaries

For anodic dissolution or cathodic deposition, the shape of an electrode changes with time. The local change in the electrode shape is related to the local current density through

$$\frac{\partial h_n}{\partial t} = \frac{M}{nF\rho}\, i_n, \tag{12}$$

where h_n is the distance normal to the surface. Wagner [40] gave an analytic solution for an electropolishing process applied to an initial surface with low amplitude, sinusoidal roughness. His analysis assumes

that the current density is mass-transfer limited, but, since convection and migration are ignored, Laplace's equation applies. Fedkiw [41] extended Wagner's results by carrying out a regular perturbation in the ratio of the amplitude to wavelength.

Most of the other analyses are numerical. Alkire *et al.* [42] simulated with finite element methods the growth of an electrode that is initially coplanar with an insulating surface. Riggs *et al.* [43] modeled shape change during a high-rate electrochemical machining process. Prentice and Tobias [44] simulated deposition onto a corner electrode and into a wedge where the angle of intersection between the electrode and insulator is acute. Other interesting studies include papers by Deconinck *et al.* [45] and Hume and coworkers [46].

Linear stability analyses are used to predict the initial rate of growth of an irregular surface. Particular emphasis has been placed on dendrite growth. In these problems, in addition to the surface overpotential caused by the faradaic reaction, it is necessary to include the stabilizing effects of the "capillarity overpotential," which accounts for changes in the surface free energy with the radius of curvature. Landau [47] and Barkey and coworkers [48], [49] reviewed this literature. In the analysis of Barkey *et al.*, which is applied to copper deposition on rotating cylinders, Laplace's equation is solved for the potential and for the concentration of the reacting species. The two fields are coupled through Faraday's law and the concentration overpotential. Their results generalize the analyses of Wagner [40], Landau [47], and Aogaki and Makino [50]. A classic analysis concerned with the initial growth of dendrites was given by Mullins and Sekerka [51].

Details about proceeding with linear stability analyses can be found in the fluid-mechanics literature (see, for example, White [52]).

3. Solution Methods

3.1. Numerical Methods

Klingert, Lynn, and Tobias [53] were the first to study numerically current distributions. Fleck [10] discussed the use of finite-difference methods for determining current distributions. Many other techniques have been used and were reviewed by Prentice and Tobias [7]. Since their review, the trend in solving for current distributions has been towards using finite-element methods and techniques based on Green's second theorem (for example, boundary-element methods). These techniques provide the greatest flexibility for solving Laplace's equation in geometries that can not be mapped into a rectangular domain. A general discussion of finite-element methods can be found, for example, in references [54] or [55]. Discussions of boundary-element methods are found in references [56], [57], and [58].

Within the context of current distribution problems, Dukovic [34] discussed the relative advantages of the two methods. Hume *et al.* [59] compared finite-element and boundary-element methods as they are applied to a moving boundary problem. Matlosz *et al.* [60] used both techniques to calculate the secondary current distribution in a Hull cell. Cahan *et al.* [61] introduced a procedure based on Green's theorem. Previously, Alkire and Mirarefi [6], and Newman and coworkers [3], [5], [9], [14], [62] used numerical methods based on Green's theorem.

Morris and Smyrl [63] used finite-element methods for a three-dimensional study of galvanic interactions on heterogeneous surfaces. In a subsequent paper, Morris and Smyrl [64] gave current distributions on irregular, heterogeneous surfaces that were numerically created with Voronoi tessellations. A major result of this and their previous paper is that the simulation of an axisymmetric, disk inclusion elucidates much of the important behavior of galvanic interactions. Consequently, for many applications, three-dimensional simulations are unnecessary. Shih and Pickering [65] used a technique based on Green's theorem for a three-dimensional study of the current distribution on a square electrode imbedded in an insulating plane. Zamani *et al.* [66] reviewed the modeling of cathodic protection systems. They emphasized, that for practical geometries, finite-element and boundary-element methods are more useful than finite-difference methods. They discuss both two and three-dimensional studies, and conclude that, for three-dimensional geometries, boundary-element methods are preferred because of the difficulties in generating a three-dimensional, finite-element grid.

General software for solving Laplace's equation is popular. For the simulation of certain cases (for example, systems with large polarization parameters), these programs are expected to provide solutions of low accuracy. Nevertheless, general software can be useful for these problems because, often, high accuracy is not necessary. With insight from asymptotic solutions and analytic techniques, the computer code (or the problem formulation) can be modified to enhance the accuracy.

Computers also permit more information to be obtained from procedures that are mainly analytic. A series solution, for example, pro-

vides little information unless it is evaluated numerically, and its results are displayed graphically. Orazem and Newman [67] and Diem *et al.* [68] used a computer with Schwarz-Christoffel transformations to evaluate numerically the resulting integrals. A formal solution, without this numerical evaluation, would be of little value.

3.2. Coordinate Transformations

Most researchers are, at least, familiar with the outcome of coordinate transformations for they have undoubtedly been exposed to cylindrical or spherical coordinate systems. A goal of such transformations is to find coordinates for which the boundary conditions can be expressed easily. Hence, for simple cases, an analytic solution can be attained. Newman [9] discussed extensively coordinate transformations; therefore our treatment is brief. As an example, he used rotational-elliptic coordinates, shown in figure 3, to demonstrate how the disk-electrode system can be mapped into a rectangular geometry. Since the mapping is not conformal, the form of Laplace's equation changes and is also given in figure 3. We present here a coordinate system, which has also found use in some electrochemical systems.

Tangent-sphere coordinates were utilized to solve for the AC frequency dispersion on a mercury drop at the end of a capillary [39]. The coordinates are defined by

$$r = \frac{2r_o\mu}{\mu^2 + \nu^2} \qquad z = \frac{2r_o\nu}{\mu^2 + \nu^2}, \tag{13}$$

where r_o is the radius of the mercury drop. Because of the symmetry of the problem, there is no θ dependence. The derivatives of potential with respect to the cylindrical coordinates are related to the

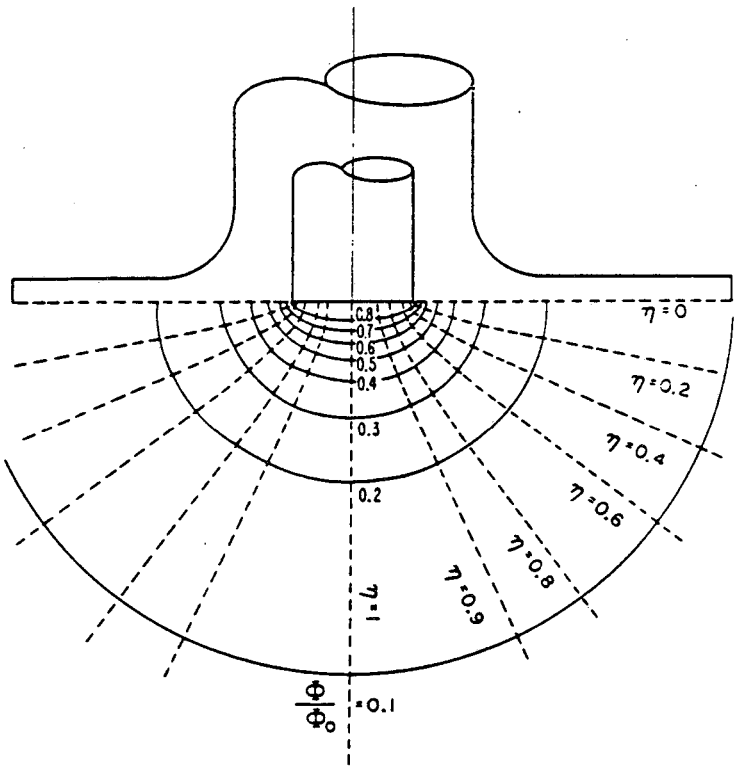

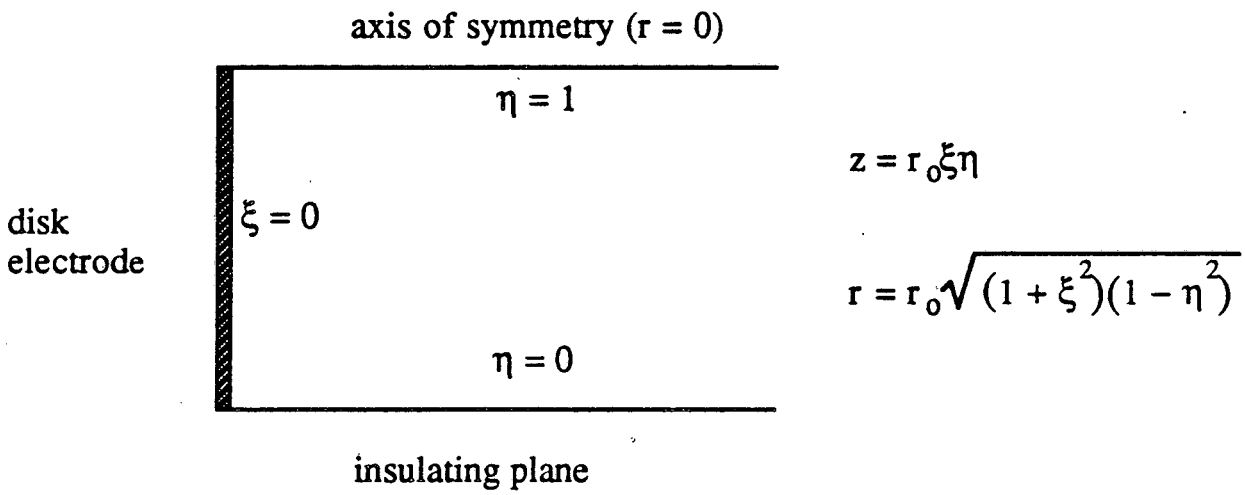

Figure 3. A schematic of the rotating-disk-electrode system, shown in the original coordinate system and in a space defined by the rotational-elliptic coordinates, where Laplace's equation is

$$\frac{\partial}{\partial \xi}\left((1+\xi^2)\frac{\partial \Phi}{\partial \xi}\right) + \frac{\partial}{\partial \eta}\left((1-\eta^2)\frac{\partial \Phi}{\partial \eta}\right) = 0$$

derivatives with respect to the new variables through

$$\frac{\partial \Phi}{\partial r} = \frac{\partial \Phi}{\partial \mu}\frac{\partial \mu}{\partial r} + \frac{\partial \Phi}{\partial \nu}\frac{\partial \nu}{\partial r} = \frac{-1}{r_o}\left[\frac{\mu^2 - \nu^2}{2}\frac{\partial \Phi}{\partial \mu} + \mu\nu\frac{\partial \Phi}{\partial \nu}\right], \tag{14}$$

and

$$\frac{\partial \Phi}{\partial z} = \frac{-1}{r_o}\left[\frac{\nu^2 - \mu^2}{2}\frac{\partial \Phi}{\partial \nu} + \mu\nu\frac{\partial \Phi}{\partial \mu}\right], \tag{15}$$

Following this procedure the second derivatives can be determined. The substitutions are straightforward, but the algebra can be laborious. With these substitutions, Laplace's equation becomes

$$\frac{\partial}{\partial \mu}\left[\frac{\mu}{\mu^2 + \nu^2}\frac{\partial \Phi}{\partial \mu}\right] + \frac{\partial}{\partial \nu}\left[\frac{\mu}{\mu^2 + \nu^2}\frac{\partial \Phi}{\partial \nu}\right] = 0. \tag{16}$$

Sides and Tobias [69] also used tangent-sphere coordinates to describe the primary current distribution around an attached, insulating bubble. Moon and Spencer [70] provided a compilation of coordinate systems. They also gave Laplace's equation written in terms of the new coordinates. For some situations, conformal mapping, discussed below, is valuable for providing new coordinate systems.

3.3. Conformal Mapping

Moulton [71] used conformal mapping to solve for the primary current distribution on two electrodes placed at arbitrary positions on an otherwise insulating rectangle. Fleck [10] and Kojima [11] gave electrochemical cells to which conformal mapping procedures have been applied. Unless it is coupled with other methods, conformal mapping is limited in its use to primary current distributions in two-dimensional geometries. Most texts that discuss the applications of complex variables explain conformal mapping (see, for example, Churchill [72]).

The goal of conformal mapping is to map a geometry into one in which the solution is known. The form of Laplace's equation always remains the same,

$$\frac{\partial^2 \Phi}{\partial u^2} + \frac{\partial^2 \Phi}{\partial v^2} = 0, \tag{17}$$

where u and v are the new coordinates. Orazem and Newman [67] mapped the geometry shown in figure 4a into the rectangle shown in figure 4c. The coordinate system shown in figure 4b is an intermediate geometry used in the solution procedure. The mappings are obtained by a Schwarz-Christoffel transformation, which maps a straight line into a polygon.

To demonstrate conformal mapping, we discuss how the current distribution on a recessed electrode deviates from the current distribution of an electrode that is coplanar with an insulating plane. The problem may be important, for example, for electroplating processes common in the electronics industry. Figure 5a shows the geometry of interest. Wagner [23] gave the current distribution for a zero aspect ratio ($m/n = 0$):

$$\frac{i(x)}{i_{avg}} = \frac{2}{\pi}(1 - x^2/n^2)^{-1/2} . \tag{18}$$

The counterelectrode can be considered a hemicylinder placed very far from the working electrode. To obtain a solution, the cell is mapped into the geometry shown in figure 5c; figure 5b shows an intermediate coordinate system that is used in the mapping. These coordinates are related through

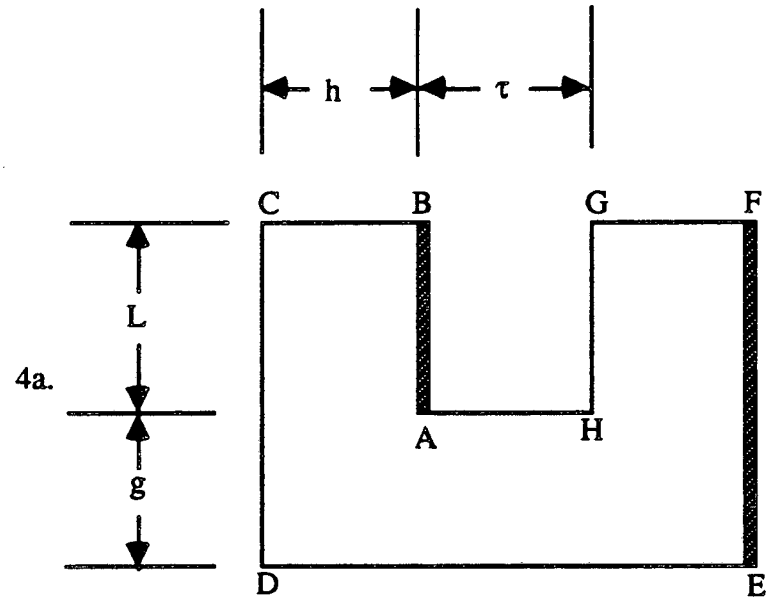

4a.

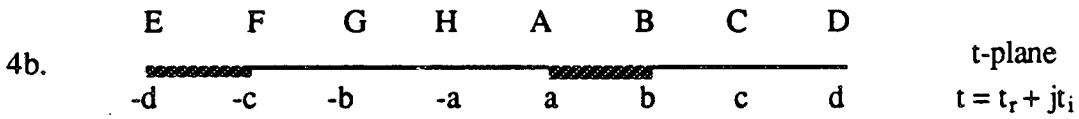

4b.

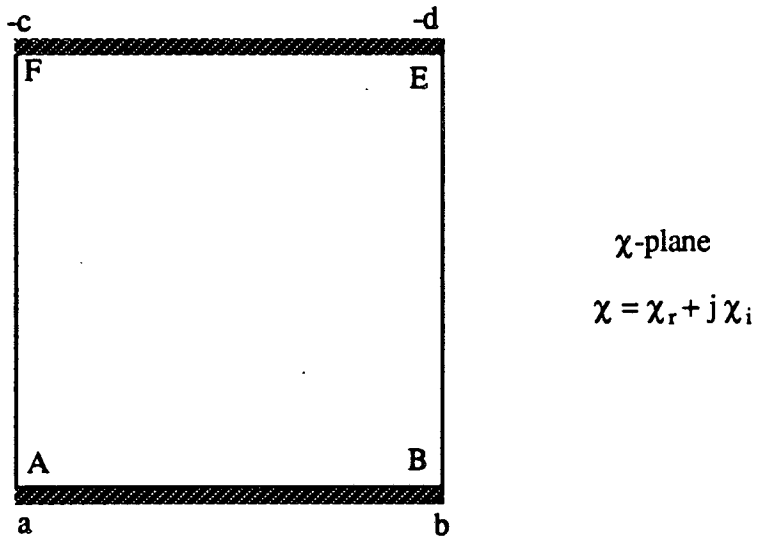

4c.

Figure 4. Schematic diagram of a slotted-electrode cell. Figure 4a shows the cell in the original coordinate system. To facilitate solution of Laplace's equation it is mapped conformally to the coordinate system of figure 4c, with the coordinate system shown in figure 4b as an intermediate coordinate system. See reference [67] for details.

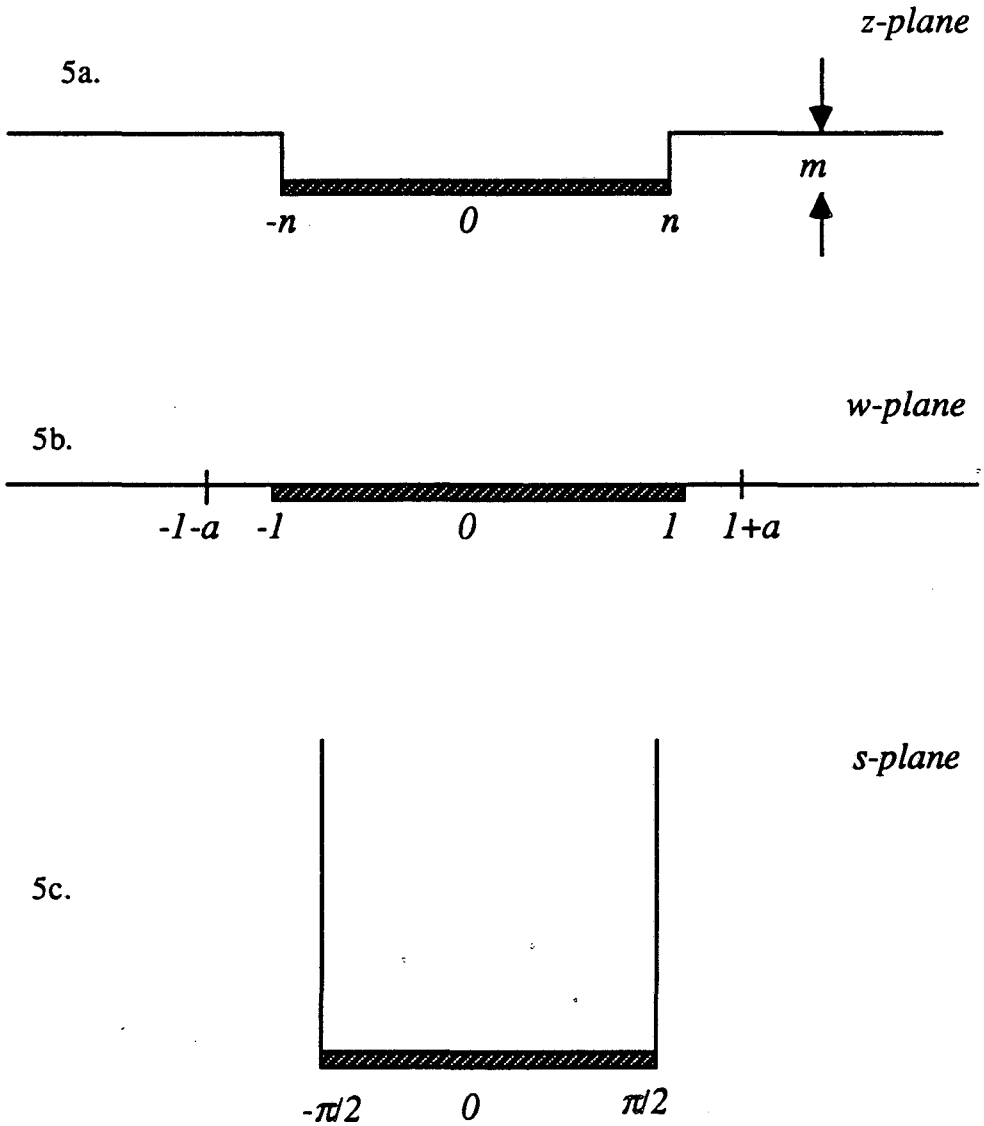

Figure 5. A schematic of the mappings used to determine the ohmic resistance of a recessed, planar electrode, with a counterelectrode placed at a distance very far from the working electrode.

$$\frac{dz}{dw} = C \frac{\sqrt{w-1-a}\ \sqrt{w+1+a}}{\sqrt{w-1}\ \sqrt{w+1}}, \tag{19}$$

and

$$w = \sin(s). \tag{20}$$

The constants a and C can be related to m and n by integrating equation (19):

$$m = C \int_{1}^{1+a} \left[\frac{(1+a)^2 - w^2}{w^2 - 1} \right]^{1/2} dw \tag{21}$$

and

$$n = C\ (1+a)\ E[(1+a)^{-2}], \tag{22}$$

where $E[(1+a)^{-2}]$ is the complete elliptic integral of the second kind, as defined by Abramowitz and Stegun [73].

The solution to Laplace's equation in the s-plane is

$$\Phi = \frac{\Phi_c}{s_c} s_i, \tag{23}$$

where Φ_c is the potential of the counterelectrode, the potential of the working electrode is set to zero, and s_c specifies the location of the counterelectrode in the s-plane. The current distribution in the w-plane is given by

$$\frac{\partial \Phi}{\partial w_i} = \frac{\partial \Phi}{\partial s_i} \frac{\partial s_i}{\partial w_i} + \frac{\partial \Phi}{\partial s_r} \frac{\partial s_r}{\partial w_i}. \tag{24}$$

Equation (23) shows that the second term on the right side of equation (24) is zero. The Cauchy-Riemann conditions,

$$\frac{\partial s_i}{\partial w_i} = \frac{\partial s_r}{\partial w_r} \quad ; \quad \frac{\partial s_i}{\partial w_r} = - \frac{\partial s_r}{\partial w_i}, \tag{25}$$

can be used show that

$$\frac{\partial \Phi}{\partial w_i} = \frac{\Phi_c}{s_c} (1 - w_r^2)^{-\frac{1}{2}} . \tag{26}$$

Following the same procedure for the z-plane,

$$\frac{\partial \Phi}{\partial z_i} = \frac{1}{C} \frac{\Phi_c}{s_c} ((1+a)^2 - w_r^2)^{-\frac{1}{2}} . \tag{27}$$

For small m/n, the constants introduced in equation (19) are determined through

$$m = \frac{\pi}{2} aC \tag{28}$$

and

$$n = C[1 - \frac{a}{2} \ln(a)]. \tag{29}$$

Furthermore, it can be shown for small m/n that

$$\frac{i(z_r=n)}{i_{avg}} = \frac{\sqrt{n/m}}{\sqrt{\pi}}, \tag{30}$$

and, at the center of the electrode,

$$\frac{i(z_r=0)}{i_{avg}} = \frac{2}{\pi} \left[1 - \frac{1}{\pi} \frac{m}{n} \ln(m/n)\right]. \tag{31}$$

Equation (30) shows how an infinite current density is approached when the aspect ratio goes to zero, and the second term on the right side of equation (31) shows that, for small aspect ratios, the current distribution near the center of the electrode is adequately described by the current distribution for zero m/n.

The ohmic resistance of this cell is given by

$$W\kappa R = \frac{s_c}{\pi} , \tag{32}$$

where W is the width of the cell (perpendicular to the page). For $m/n = 0$, since $s_c = \ln(2z_c/n)$, the ohmic resistance is given by

$$W\kappa R_o = \frac{\ln(2z_c/n)}{\pi}. \tag{33}$$

The deviation from this resistance, for small m/n, is

$$W\kappa R - W\kappa R_o = -\frac{1}{\pi^2}\frac{m}{n}\ln(m/n). \tag{34}$$

Equations (30), (31) and (34) are asymptotically valid for small m/n. The current distribution and ohmic resistance for a cell similar to this one was investigated by Diem *et al.* [68]. Their analysis can be used to indicate when this predicted behavior is valid. West and Newman [74] gave a singular-perturbation analysis that shows more generally the characteristics of recessed electrodes for small aspect ratios.

3.4. Separation of Variables

For some cells with sufficiently simple boundary conditions, a solution can be obtained by the method of separation of variables. For such a solution to be possible, the boundary conditions must be linear, and all but one must be homogeneous. Most texts on partial differential equations discuss this technique (for example, see reference [12] or [75]). Both Ibl [8] and Newman [9] used the disk-electrode geometry as an example to demonstrate the method of separation of variables.

It should also be realized that, for some coordinate systems, a less trivial solution must be proposed. Moon and Spencer [70] gave solutions that can be "guessed" to solve Laplace's equation. In the tangent-sphere coordinate system defined earlier we would set

$$\Phi = (\mu^2 + \nu^2)^{\frac{1}{2}} M(\mu)N(\nu). \tag{35}$$

Substituting this guess into equation (16) verifies that a solution of this form is separable, although it might not satisfy the boundary

conditions.

We discuss here problems that can be solved without much complicated algebra. The first problem is concerned with the potential distribution in a mercury-pool electrolysis cell at the limiting current. Its solution was originally given by Newman and Harrar [76].

Figure 6 shows the geometry that is being modeled. Laplace's equation in cylindrical coordinates is

$$\frac{1}{r}\frac{\partial}{\partial r}\left(r\frac{\partial \Phi}{\partial r}\right) + \frac{\partial^2 \Phi}{\partial z^2} = 0. \tag{36}$$

The boundary conditions are

$$\frac{\partial \Phi}{\partial z} = -\frac{i_{avg}}{\kappa} \quad \text{at } z = 0, \tag{37}$$

$$\frac{\partial \Phi}{\partial r} = 0 \quad \text{at } r = r_w, \tag{38}$$

$$\frac{\partial \Phi}{\partial z} = -\frac{i_{avg}}{\kappa}\frac{r_w^2}{r_c^2} \quad \text{at } z = h,\ r \le r_c, \tag{39}$$

and

$$\frac{\partial \Phi}{\partial z} = 0 \quad \text{at } z = h,\ r > r_c. \tag{40}$$

Because the boundary conditions specified at $z = 0$ and $z = h$ are both nonhomogeneous, a separation of variables solution is not possible. By solving instead for Ψ, where

$$\Psi = \Phi - \frac{i_{avg}}{\kappa} z, \tag{41}$$

the boundary condition at $z = 0$ becomes a homogeneous, insulator condition. At $z = h$, the boundary condition is

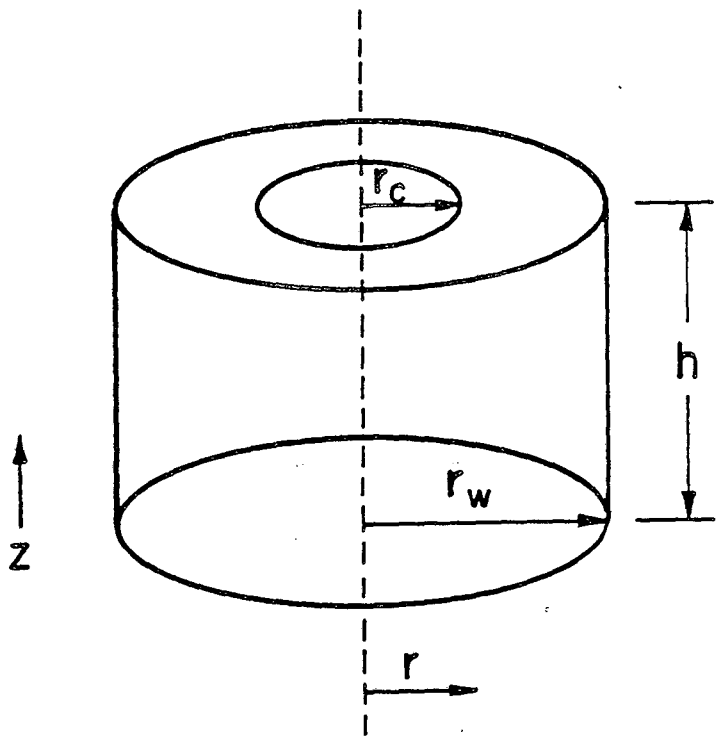

Figure 6. Axisymmetric cylindrical cell with the working electrode at the bottom and the counterelectrode at the top (taken from reference [76]).

$$\frac{\partial \Psi}{\partial z} = \frac{i_{avg}}{\kappa}\left[\frac{r_w^2}{r_c^2} - 1\right] \quad \text{for } r \le r_c, \tag{42}$$

and

$$\frac{\partial \Psi}{\partial z} = -\frac{i_{avg}}{\kappa} \quad \text{for } r > r_c. \tag{43}$$

We now assume that $\Psi(r,z) = R(r)Z(z)$, substitute into equation (36), and obtain the following ordinary differential equations:

$$\frac{\partial^2 R}{\partial r^2} + \frac{1}{r}\frac{\partial R}{\partial r} + \lambda_n^2 R = 0 \tag{44}$$

and

$$\frac{\partial^2 Z}{\partial z^2} - \lambda_n^2 Z = 0. \tag{45}$$

λ_n is a constant that arises because separation of variables is possible and will be determined from the boundary conditions. The solution to equation (44), when the insulator boundary condition at $r = r_w$ is applied, is

$$R(r) = A_n J_o(\lambda_n \frac{r}{r_w}), \tag{46}$$

where J_o is the Bessel function of the first kind of order zero, and λ_n is the n^{th} root of $J_1(x)$. The solution to equation (45) that satisfies the insulating boundary condition at $z = 0$ is

$$Z(z) = B_n \cosh(\lambda_n \frac{z}{r_w}). \tag{47}$$

Since an infinite number of λ_n satisfy the above equations, Ψ can be written as

$$\Psi = -\frac{i_{avg} r_w}{\kappa} \sum_{n=1}^{\infty} C_n \cosh(\lambda_n \frac{z}{r_w}) J_o(\lambda_n \frac{r}{r_w}). \tag{48}$$

Functions that satisfy Sturm-Liouville problems, such as equation (44) and its boundary conditions, are orthogonal. That is, if the solutions to the problem are ϕ_n and the boundary conditions are specified at a and b, then

$$0 = \int_a^b \phi_n(x)\phi_m(x)w(x)dx \quad \text{for } m \neq n. \tag{49}$$

$w(x)$ is a weighting function defined by Hildebrand [77]. For equation (44) the weighting function is r. Using the orthogonality condition, we conclude that the last boundary condition is satisfied if

$$C_n = \frac{2\,\frac{r_w}{r_c}\,J_1(\lambda_n\,\frac{r_c}{r_w})}{\lambda_n^2\,[J_o(\lambda_n)]^2\sinh(\lambda_n h/r_w)}\,. \tag{50}$$

This problem may also be of interest for cathodic protection, where it is important to know the maximum potential variation along an electrode. The results could be compared with equation (3), which gives the maximum potential difference for an isolated disk electrode. Newman and Harrar [76] discussed the influence of the geometric ratios r_w/r_c and h/r_w on the potential variations on the working electrode. It may also be interesting to calculate how the potential along the counterelectrode varies. Pierini and Newman [15] showed how the geometric ratios affect the ohmic resistance of this cell.

Figure 7 shows another geometry and set of boundary conditions for which the solution can be obtained from separation of variables. For now, we will not consider whether this problem statement is physically realistic. The mathematics will eventually confirm our intuition that it is not.

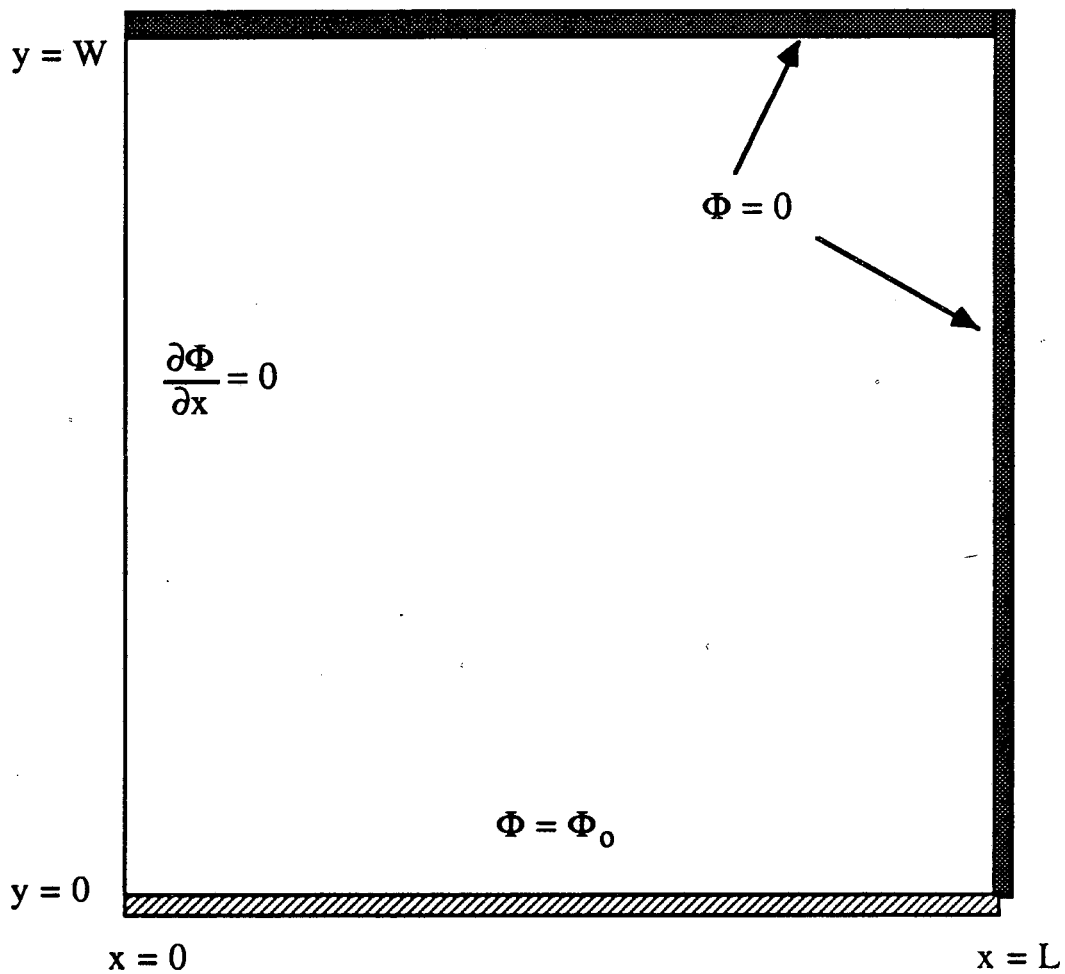

Figure 7. Two electrodes at different potentials placed into contact with one another.

The solution to this problem in cartesian coordinates is

$$\Phi(x,y) = \sum_{n=1}^{\infty} (-1)^n \frac{-2\Phi_o}{\pi(n - 1/2)} \cos(\lambda_n x) \frac{\sinh(\lambda_n(W - y))}{\sinh(\lambda_n W)}. \qquad (51)$$

We often desire the current density along the working electrode:

$$i_n(x,0) = -\kappa \left.\frac{\partial\Phi}{\partial y}\right|_{y=0} = \frac{2\kappa\Phi_o}{L} \sum_{n=1}^{\infty} \frac{\sin(\lambda_n(L - x))}{\tanh(\lambda_n W)} . \qquad (52)$$

This series does not converge, although this may not be obvious without a close inspection. In fact, the series solution gives no insight into how the current density behaves near the singular point $x = L$, $y = 0$. In the next section, a technique that provides this insight is discussed.

3.5. Similarity Transformations

Similarity transformations are useful for elucidating the current distribution at short times or near singular points in space. Similarity solutions for various situations are given by Sedov [78].

To demonstrate the method and its usefulness, we explore the nature of the singularity that is discussed at the end of the previous section. Sufficiently close to the singular point, the location of the other boundaries is unimportant. Hence, the current distribution near $x = L$, $y = 0$ is expected to be independent of the characteristic lengths L and W. In this region, then, one might assume that

$$\frac{\Phi}{\Phi_o} = f(\eta), \qquad (53)$$

where $\eta = y/(L-x)$. Since the second derivatives expressed in terms of these variables are

$$\frac{1}{\Phi_o}\frac{\partial^2\Phi}{\partial x^2} = \frac{d^2f}{d\eta^2}\left(\frac{\partial\eta}{\partial x}\right)^2 + \frac{df}{d\eta}\frac{\partial^2\eta}{\partial x^2} = \frac{1}{(L-x)^2}\frac{d^2f}{d\eta^2} \tag{54}$$

and

$$\frac{1}{\Phi_o}\frac{\partial^2\Phi}{\partial y^2} = \frac{2\eta}{(L-x)^2}\frac{df}{d\eta} + \frac{\eta^2}{(L-x)^2}\frac{d^2f}{d\eta^2}, \tag{55}$$

Laplace's equation can be written as

$$(1+\eta^2)\frac{d^2f}{d\eta^2} + 2\eta\frac{df}{d\eta} = 0. \tag{56}$$

For the similarity transformation to work, the boundary conditions must also be functions only of η. For this case, they are

$$f = 1 \quad \text{at} \quad \eta = 0 \quad \text{and} \quad f \longrightarrow 0 \quad \text{as} \quad \eta \longrightarrow \infty. \tag{57}$$

Equation (56) is a Legendre equation of imaginary argument of order zero and has the solution

$$\frac{\Phi}{\Phi_o} = f(\eta) = 1 - \frac{2}{\pi}\tan^{-1}\eta. \tag{58}$$

The current density along the working electrode near the singular point is given by

$$i_n(x) = -\kappa\left.\frac{\partial\Phi}{\partial y}\right|_{y=0} = -\frac{\kappa\Phi_o}{L-x}\left.\frac{df}{d\eta}\right|_{\eta=0} = \frac{2}{\pi}\frac{\kappa\Phi_o}{L-x}. \tag{59}$$

The current density given by equation (59) is infinite at $x = L$. For all physical situations, the current density remains finite because the kinetic resistance is never quite zero. Nevertheless, for some cases, a current distribution is approximately correct over most of the electrode despite the singularity. Depending on the application, such current distributions are not too bothersome because they contain "integrable" singularities, and may in some sense display the correct average behavior. The singularity of equation (59) is called

nonintegrable because the total current is infinite. The model, then, is of no practical use, and our intuition is confirmed that two conductors in physical contact with one another can not be set at different potentials.

A current distribution containing a singularity of the form $i(x) \propto x^{-n}$ as $x \longrightarrow 0$ is integrable if $n < 1$. Equation (80) shows that the singularity that occurs in most primary current distribution calculations is integrable. This indicates that the assumptions leading to this equation, while not strictly correct, are, at least, more realistic than the situation modeled here.

Similarity transformations might find greater use for equations other than Laplace's. For example, they are of great utility for transient-diffusion problems [12] and for boundary-layer theory [79]. The method is discussed here because it is useful to develop devices for thinking about asymptotic behavior. Being comfortable with similarity transformations will help one master, for example, singular perturbation techniques.

To summarize, similarity transformations involve the combination of the independent variables, resulting in an ordinary differential equation, which must be solved instead of a partial differential equation. For such a procedure to work, it is necessary that the boundary conditions can be combined and expressed consistently in terms of the similarity variable and that the original, independent variables do not appear explicitly in the ordinary differential equation.

3.6. AC Impedance Analyses

Laplace's equation sometimes arises in the explanation of AC impedance data. Newman [39] showed how nonuniform current distributions can cause frequency dispersion on a disk electrode. Jakšić and Newman [80] later showed that this model satisfies the Kramers-Kronig relations. Glarum [81] also solved for the frequency dispersion on a disk electrode to show the usefulness of variational approximations. Glarum and Marshall [82] used these results to interpret experimental data. To quantify frequency dispersion caused by surface roughness, the frequency response of electrodes with fractal roughness has been investigated [83], [84], [85].

We demonstrate how AC impedance analyses are carried out. First, it is necessary to determine the steady-state current distribution so that a linear analysis of the frequency response is possible. For our purposes, we assume that it is described by Laplace's equation. The boundary conditions everywhere except the working electrode are homogeneous and, hence, uninteresting. Along the working electrode, we assume Tafel kinetics:

$$i(x) = -\kappa \frac{\partial \Phi}{\partial y} = i_o \exp\left[\frac{\alpha_a F}{RT} (V - \Phi_o)\right] + C \frac{\partial (V - \Phi_o)}{\partial t}, \qquad (60)$$

where the last term is zero for the steady-state solution.

To carry out an AC impedance analysis, a small-amplitude, sinusoidal perturbation is placed on the electrode potential:

$$V = V_{ss} + \mathrm{Re}\left\{\bar{V} e^{j\omega t}\right\}, \qquad (61)$$

where Re{x} is the real part of the complex variable x and $\bar{V}$ is a real

constant. To determine the transient current distribution in response to this perturbation, it is convenient to split the potential into its steady-state and transient parts:

$$\Phi = \Phi_{ss} + \mathrm{Re}\left\{\tilde{\Phi}(x,y)e^{j\omega t}\right\}. \tag{62}$$

Because the value of $\tilde{V}$ is very small, $\tilde{\Phi}$ is also small. Since Φ_{ss} satisfies Laplace's equation, $\tilde{\Phi}$ must also satisfy it. When the steady-state potential and current distributions are subtracted from the electrode boundary condition, the boundary condition for $\tilde{\Phi}$, after it is justifiably linearized, becomes

$$-\kappa \frac{\partial \tilde{\Phi}}{\partial y} = \left[\frac{\alpha_a F}{RT} i_{ss}(x) + j\omega C\right](\tilde{V} - \tilde{\Phi}_o) , \tag{63}$$

where $i_{ss}(x)$ is the steady-state current distribution.

Finally, we can solve Laplace's equation for the real and imaginary parts of $\tilde{\Phi}$. They are coupled through

$$-\kappa \frac{\partial \tilde{\phi}_r}{\partial y} = \frac{\alpha_a F i_{ss}(x)}{RT} (\tilde{V} - \tilde{\phi}_{r,o}) + \omega C \tilde{\phi}_{i,o} \tag{64}$$

and

$$-\kappa \frac{\partial \tilde{\phi}_i}{\partial y} = -\frac{\alpha_a F i_{ss}(x)}{RT} \tilde{\phi}_{i,o} + \omega C(\tilde{V} - \tilde{\phi}_{r,o}) . \tag{65}$$

A similar analysis could be carried out for a sinusoidal, small-amplitude perturbation of the average current density. Because of the linearity of the analysis, the complex impedance will be the same. Tribollet and Newman [86], [87] outlined the correct solution procedure when concentration variations exist, and the more general transport equations must be solved.

3.7. Boundary Integral Techniques

As discussed in section 3.1, numerical techniques based on Green's second theorem are popular. Newman [9] discussed the use of these methods for the disk electrode. In this section, we present the necessary equations for developing numerical methods for two-dimensional, three-dimensional, and axisymmetric geometries.

Boundary integral methods are based on the second form of Green's theorem

$$\int_V \left(g\nabla^2\Phi - \Phi\nabla^2 g\right) dV = \int_{\partial V} \mathbf{n}\cdot\left(g\nabla\Phi - \Phi\nabla g\right) dA. \tag{66}$$

A clever choice of g greatly facilitates the determination of the potential. Specifically, g is chosen to satisfy

$$\nabla^2 g = \delta(x-x_q, y-y_q, z-z_q), \tag{67}$$

where δ is the three-dimensional Dirac delta function, x, y, and z are the cartesian coordinates, and x_q, y_q, z_q specifies a point. A Green's function g that satisfies equation (67) is $g = 1/\xi_3$, where

$$\xi_3 = \left[(x-x_q)^2 + (y-y_q)^2 + (z-z_q)^2\right]^{1/2}. \tag{68}$$

Physically, g can be thought of as the potential at x_q, y_q, z_q due to a point source of current at x, y, z.

If Φ satisfies Laplace's equation, substitution of g into equation (66) gives

$$-\alpha_3\Phi(x_q, y_q, z_q) = \int_{\partial V} \mathbf{n}\cdot\left(\frac{1}{\xi_3}\nabla\Phi - \Phi\nabla\frac{1}{\xi_3}\right) dA, \tag{69}$$

where α_3 is 4π for a point, x_q, y_q, z_q in the domain of the problem, 2π for a point on a smooth boundary, and zero for a point outside the

domain. For a point where the boundary does not vary in a smooth manner, α_3 is determined as shown in figure 8. The solution for Φ is now reduced to a problem on the boundary of the domain. Once the potential and current are known everywhere on the boundary, the potential can be found anywhere in the domain.

Since equation (67) is linear, solutions for g can be superposed. Specifically, if g_h satisfies Laplace's equation, $g_h + 1/\xi_3$ is also a solution. Choosing g_h so that $\mathbf{n}\cdot\nabla(g_h + 1/\xi_3) = 0$ everywhere along the boundary of the domain can reduce greatly the numerical computation necessary for a solution since equation (69) becomes

$$-\alpha_3\Phi(x_q,y_q,z_q) = \int_{\partial V} \mathbf{n}\cdot\left[\left(\frac{1}{\xi_3} + g_h\right)\nabla\Phi\right]dA. \tag{70}$$

This approach is taken, for example, by Alkire and Mirarefi [6] and has been used extensively by mathematical physicists [88]. A good discussion of these methods was given by Greenberg [89].

For two-dimensional geometries with no z dependence, an equation analogous to equation (69) can be written:

$$\alpha_2\Phi(x_q,y_q) = \int_{\partial A}\left[\frac{\Phi}{\xi_2}\frac{\partial\xi_2}{\partial n} - \ln\xi_2\frac{\partial\Phi}{\partial n}\right]d\ell, \tag{71}$$

where $\partial/\partial n$ implies the component of the gradient of the function normal to the boundary. α_2 is 2π for a point inside the domain, zero for a point outside the domain, and π for a point on a smooth boundary. Figure 8 shows α_2 for a point on a discontinuity on the surface. ξ_2 is given by

$$\xi_2 = \left[(x-x_q)^2 + (y-y_q)^2\right)\Big]^{\frac{1}{2}}. \tag{72}$$

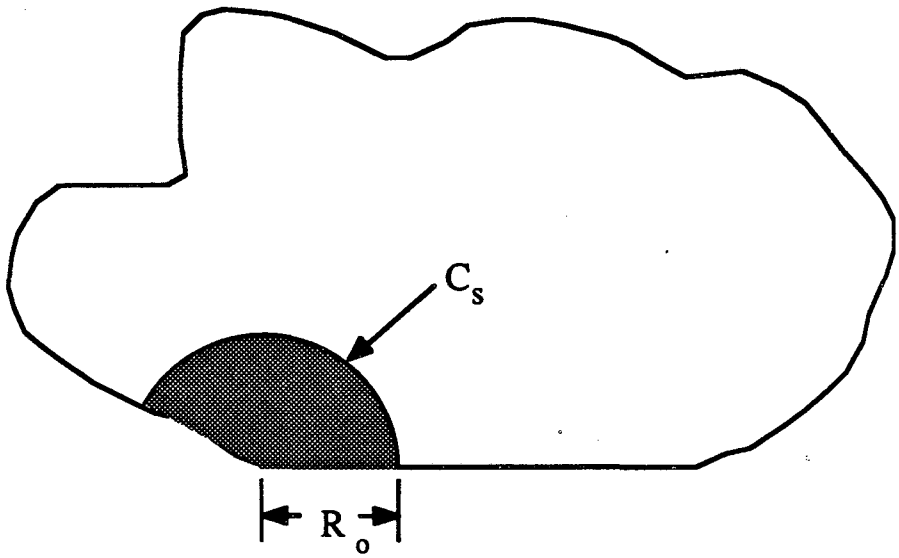

Three Dimensions

$$\alpha_3 = \lim_{R_o \to 0} \left(\frac{A_s}{R_o^2} \right)$$

Two Dimensions

$$\alpha_2 = \lim_{R_o \to 0} \left(\frac{C_s}{R_o} \right)$$

Figure 8. Schematic showing the coefficient given in equation (7) for two-dimensional geometries. A_s is the surface area of the sphere that falls within the domain of the problem, and C_s is the circumference of a circle that falls within the domain.

For axisymmetric geometries, integration of equation (69) over θ yields

$$-\alpha_3\Phi(r_q,z_q) = \int_{\partial A} \left(g \frac{\partial \Phi}{\partial n} - \Phi \frac{\partial g}{\partial n}\right) r d\ell, \tag{73}$$

where

$$g = \frac{4K(m)}{\left[(r+r_q)^2 + (z-z_q)^2\right]^{1/2}} . \tag{74}$$

$K(m)$ is the complete elliptic integral of the first kind, and

$$m = \frac{4rr_q}{(r+r_q)^2 + (z-z_q)^2} . \tag{75}$$

Tables and approximate forms of $K(m)$ are found in reference [73]. After integration over θ, $d\ell$ signifies the length element for the the path enclosing the region in the r,z half plane and n signifies a direction normal to this path. Where the path coincides with the z-axis, the integrand of equation (73) is zero.

Wrobel and Brebbia gave [90]

$$\frac{\partial g}{\partial n} = \frac{-2/r}{\left[(r+r_q)^2 + (z+z_q)^2\right]^{1/2}} \left[K(m) + \frac{r^2 - r_q^2 - (z-z_q)^2}{(r-r_q)^2 + (z-z_q)^2} E(m)\right] \mathbf{e}_r \tag{76}$$

$$- \frac{4E(m)(z-z_q)}{\left[(r+r_q)^2 + (z+z_q)^2\right]^{1/2} \left[(r-r_q)^2 + (z-z_q)^2\right]} \mathbf{e}_z ,$$

where $\mathbf{e}_r$ and $\mathbf{e}_z$ are the normal vectors in the r and z directions,† and $E(m)$ is the complete elliptic integral of the second kind. To calculate the potential in the plane of the disk electrode, equation (73) becomes [9]

$$\Phi_o(r_q) = \frac{2}{\pi\kappa} \int_0^{r_o} \frac{i_n(r)K(m)r}{r + r_q}\, dr. \tag{77}$$

3.8. Perturbation Analyses

Perturbation analyses extend results that are strictly valid when some parameter or coordinate approaches an extreme value of zero or infinity. For example, perturbation methods can elucidate the characteristics of the current distribution as the polarization parameter becomes large or small. They have also been used to describe the current distribution at short times [37] after a step change in electrode potential. A regular perturbation analysis can be used when some simplifying assumption that applies when the parameter is set to zero (or infinity) is a good approximation over the entire domain. For example, West *et al.* [24] used a regular perturbation analysis to show how the linear and Tafel current distributions deviate from a uniform current distribution when J (or δ) $\longrightarrow 0$. The analysis is regular because, when J or δ is small but nonzero, it is still true everywhere

---

† Useful relations for deriving these and similar equations are:

$$\frac{dK(m)}{dm} = -\frac{K(m)}{2m} + \frac{E(m)}{2m(1-m)}$$

and

$$\frac{dE(m)}{dm} = \frac{1}{2m}\Big[E(m) - K(m)\Big] .$$

that the local surface overpotential is very large compared to the ohmic potential drop.

For linear kinetics, when $J = 0$, the current distribution is uniform, and the ohmic potential drop is zero. Hence, Φ_o is equal to the potential at infinity, which, for this problem, is arbitrarily set equal to zero. These facts suggest that the potential is appropriately expanded as

$$\frac{\Phi}{V} = J\Phi^{(1)} + J^2\Phi^{(2)} + \ldots , \tag{78}$$

where all of the $\Phi^{(n)}$ are of order unity. Substitution of equation (78) and the linear kinetics relationship into equation (77) gives a formal solution for the potential, where terms of the same order in J are equated. Each $\Phi^{(n)}$ can be determined from equation (77), with a known integrand that has a current density determined from the $(n-1)th$ potential distribution. West *et al.* [24] gave

$$\frac{i_n}{i_{avg}} = 1 + J(\bar{\Phi}_o^{(1)} - \Phi_o^{(1)}) + J^2(\bar{\Phi}_o^{(2)} - \Phi_o^{(1)}\bar{\Phi}_o^{(1)} - \Phi_o^{(2)}) + \ldots , \tag{79}$$

where the $\bar{\Phi}_o^{(n)}$ arise as corrections to the average current density.

A similar procedure can be followed for Tafel kinetics. As Wagner [23] suggested, the first correction to a uniform current distribution is the same as for linear kinetics. For larger values of the polarization parameter, the two distributions deviate. Figure 9, taken from reference [24], shows the first-order correction to the current density at the edge and center of a disk electrode. Also shown are results calculated from the procedure described in reference [1].

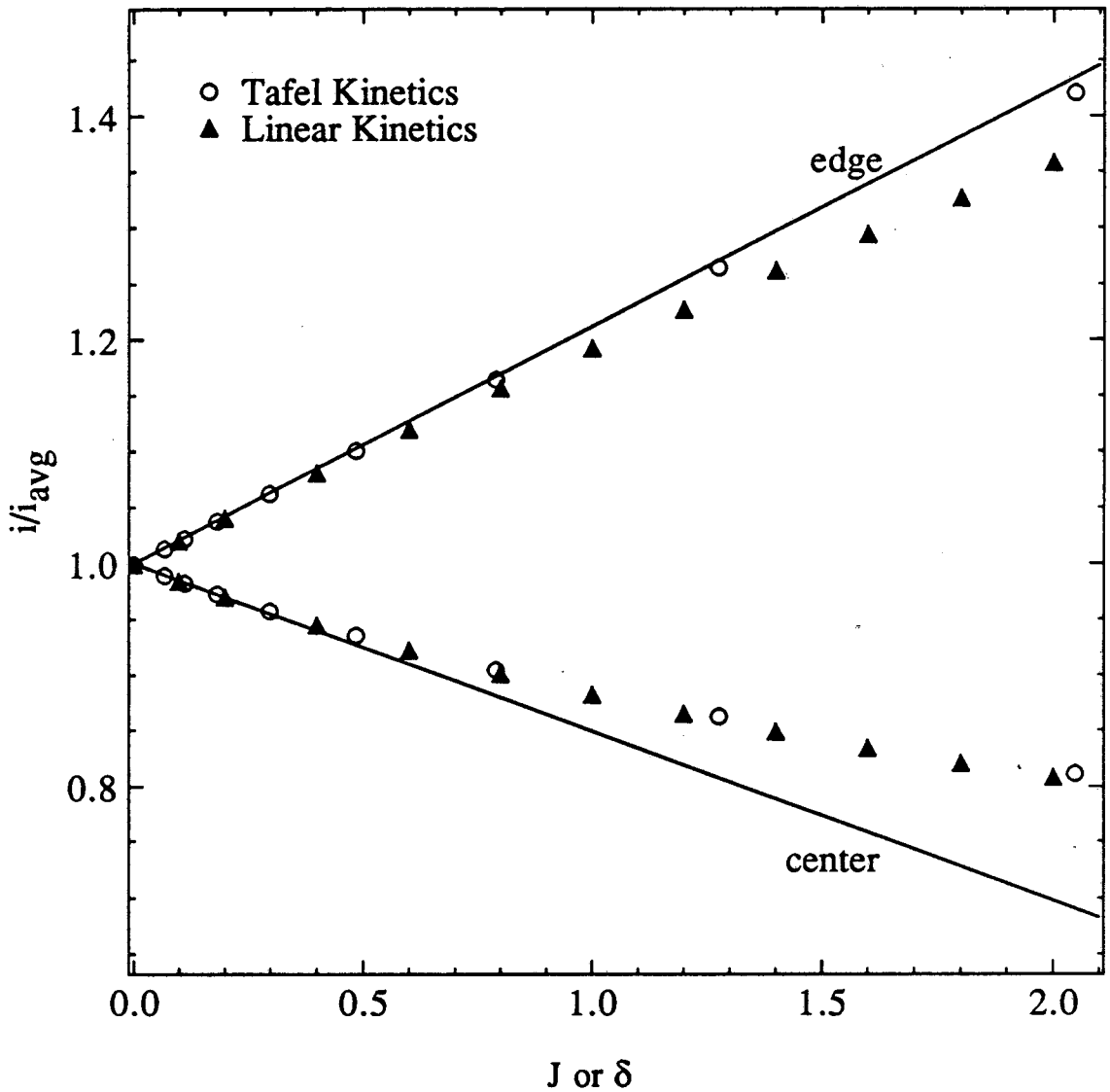

Figure 9. Calculated and predicted current densities for linear and Tafel kinetics at the center and edge of a disk electrode for small polarization parameters. For linear kinetics, the current density depends on J, and, for Tafel kinetics, it depends on δ (taken from reference [24]).

For large, finite polarization parameters, the primary current distribution can be a poor approximation near an electrode edge because the surface overpotential is no longer small when compared to the ohmic potential drop. It may, though, describe quite accurately the current distribution *away* from the edge region. This indicates that a singular perturbation treatment is necessary to elucidate how a primary current distribution is approached. Figure 10, taken from Smyrl and Newman [91], shows for the rotating disk electrode how, for large average current densities, the primary current distribution is a good approximation over most of the electrode. Smyrl and Newman [91] showed explicitly how a secondary current distribution described by Tafel kinetics approaches the primary current distribution for any geometry in which the electrode and insulator are coplanar. Nişancioğlu and Newman [37] provided similar results for linear kinetics. West and Newman [92] generalized the results for any β for linear and Tafel kinetics.

Singular perturbation analyses are interesting because they can provide more physical insight than a brute-force, numerical method. They also can give results where the more traditional numerical techniques fail. Van Dyke [93] discussed in detail singular perturbation analyses, which are sometimes called methods of matched asymptotic expansions. For more information, we also recommend references [94], [95] and [9].

4. Applications

In solving a problem numerically, it is helpful to have an idea of the general nature of the solution and perhaps of detailed behavior in certain regions. Asymptotic methods and solutions can then provide a

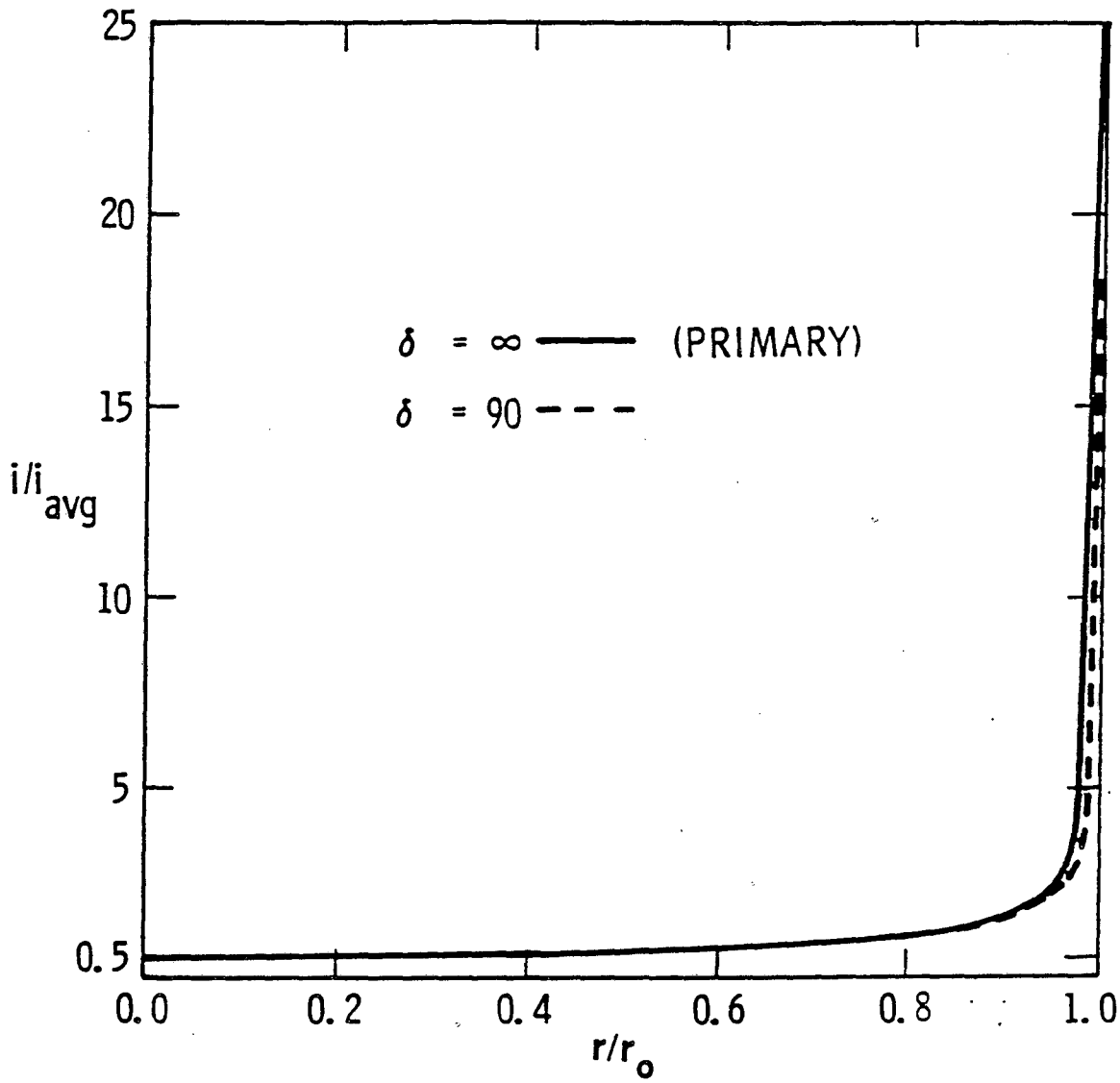

Figure 10. The primary current distribution compared to the distribution calculated for a large value of the polarization parameter for Tafel kinetics (reproduced from reference [91]).

guide in selecting numerical methods that harmonize with the inherent singularities of the problem.

4.1. Primary Current Distributions

Primary current distributions require special attention to solve numerically because they can contain current densities that are infinite at the edges of the electrodes. By solving Laplace's equation near the edge, one can show that the current density on the electrode varies as

$$i(r) = P_o r^{(\pi/2\beta - 1)}, \tag{80}$$

where r is the radial distance away from the electrode. P_o is a constant that is proportional to the average current density and is determined by specific geometric details. Equation (80) is universally true for small r for primary current distributions. The potential distribution in this region is

$$\Phi(r,\theta) = -\frac{2\beta}{\pi\kappa} P_o r^{\pi/2\beta} \sin\left(\frac{\pi\theta}{2\beta}\right). \tag{81}$$

For the rotating disk electrode, where $\beta = \pi$, a comparison of this asymptotic formula with the equation given by Newman [13]:

$$\frac{i(r)}{i_{avg}} = \frac{0.5 r_o}{(r_o^2 - r^2)^{1/2}} \tag{82}$$

would show that $P_o = \sqrt{r_o/8}\; i_{avg}$.

Numerically, it is often easier to determine a primary current distribution as a series of problems with prescribed current distributions. In this way, if a singularity exists, it can be accounted for accurately. Since the problem is linear, the resulting potential distributions can be superimposed until the constant potential boundary condi-

tion is satisfied. This technique was used to determine the current distribution on ring electrodes [62], ring-disk electrodes [5], [14], and disk electrodes in axisymmetric cylindrical cells [15]. It is particularly useful with boundary integral methods because integrable singularities are accurately evaluated if done carefully. Cabán and Chapman [96] used an orthogonal collocation procedure to calculate current distributions on plane, parallel electrodes. Villadsen and Michelson [97] also discussed collocation methods.

To determine the primary current distribution on the electrode shown in figure 11, the correct singularities at $x = 0$ and $x = L$ must be imbedded into the problem:

$$i(x) = Ax^{-1/3} + B(L - x)^{-1/2} + \sum_{n=1}^{N} C_n \psi_n(x). \tag{83}$$

The first two terms are chosen to go to infinity at the electrode edges in a manner prescribed by equation (80). The $\psi_n(x)$ are a set of orthogonal functions, and the constants A, B, and C_n are determined so that the constant potential boundary condition is satisfied. In theory, any set of orthogonal functions will work, but, in practice, some work better than others. The best choice of $\psi_n(x)$ minimizes the number of functions N necessary to satisfy the constant potential boundary condition to within a specified accuracy. The best orthogonal functions might be determined by solving a related Sturm-Liouville problem.

It is usually best to choose orthogonal functions that have the correct behavior as determined by some boundary condition or by geometric symmetry. For example, one might try to determine numerically the primary current distribution of a recessed disk electrode, shown in

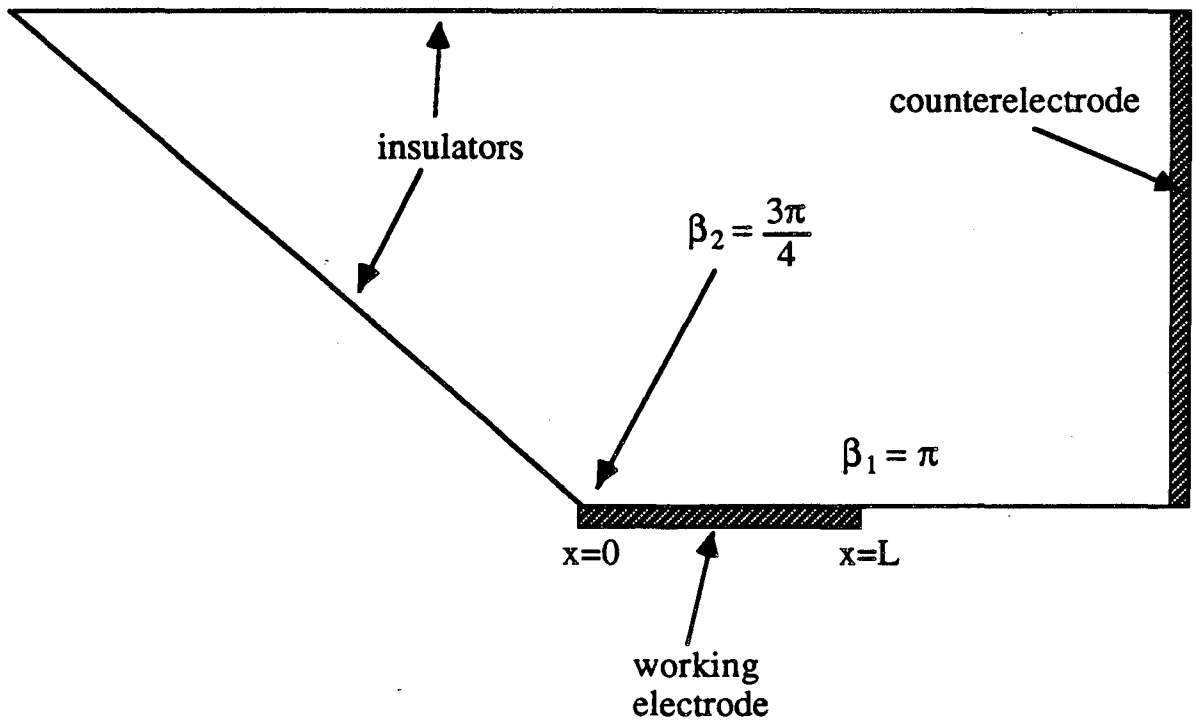

Figure 11. Schematic of a cell for which the primary current distribution might be expanded in a series given by equation (83).

figure 12. Since, at $r = 0$, $\partial P_{2n}/\partial r = 0$, one might try to superimpose even Legendre polynomials. At $r = r_o$, one needs $di_n/dr = 0$ according to equation (80). To satisfy this condition, the arguments of the function can be modified:

$$i(r) = \sum_{n=0}^{N} C_n P_{2n}\left[\sin\left(\frac{\pi r}{2r_o}\right)\right] . \tag{84}$$

An alternative series, suggested from the Sturm-Liouville problem discussed in section 3.4, is

$$i(r) = \sum_{n=0}^{N} C_n J_o(\lambda_n r/r_o) . \tag{85}$$

The λ_n are the roots of $J_1(x)$, chosen to satisfy the zero-derivative condition at $r = r_o$ [98]:

$$\left.\frac{\partial J_o(\lambda_n r/r_o)}{\partial r}\right|_{r=r_o} = -\frac{\lambda_n}{r_o} J_1(\lambda_n) . \tag{86}$$

Secondary current distributions can also be determined with these techniques, although it is no longer necessary to imbed singularities. For linear kinetics, potential distributions resulting from prescribed current distributions can be superimposed until the boundary conditions are satisfied. For Tafel or Butler-Volmer kinetics, potential distributions can still be superimposed, but determining the coefficients C_n is a nonlinear, iterative process.

4.2. Conformal Mapping

Conformal mapping procedures are useful for primary current distributions, but, alone, they are not of great utility for problems with mixed or Neumann boundary conditions. Newman [27] mapped conformally a flow-channel reactor so that its insulators and electrodes are coplanar

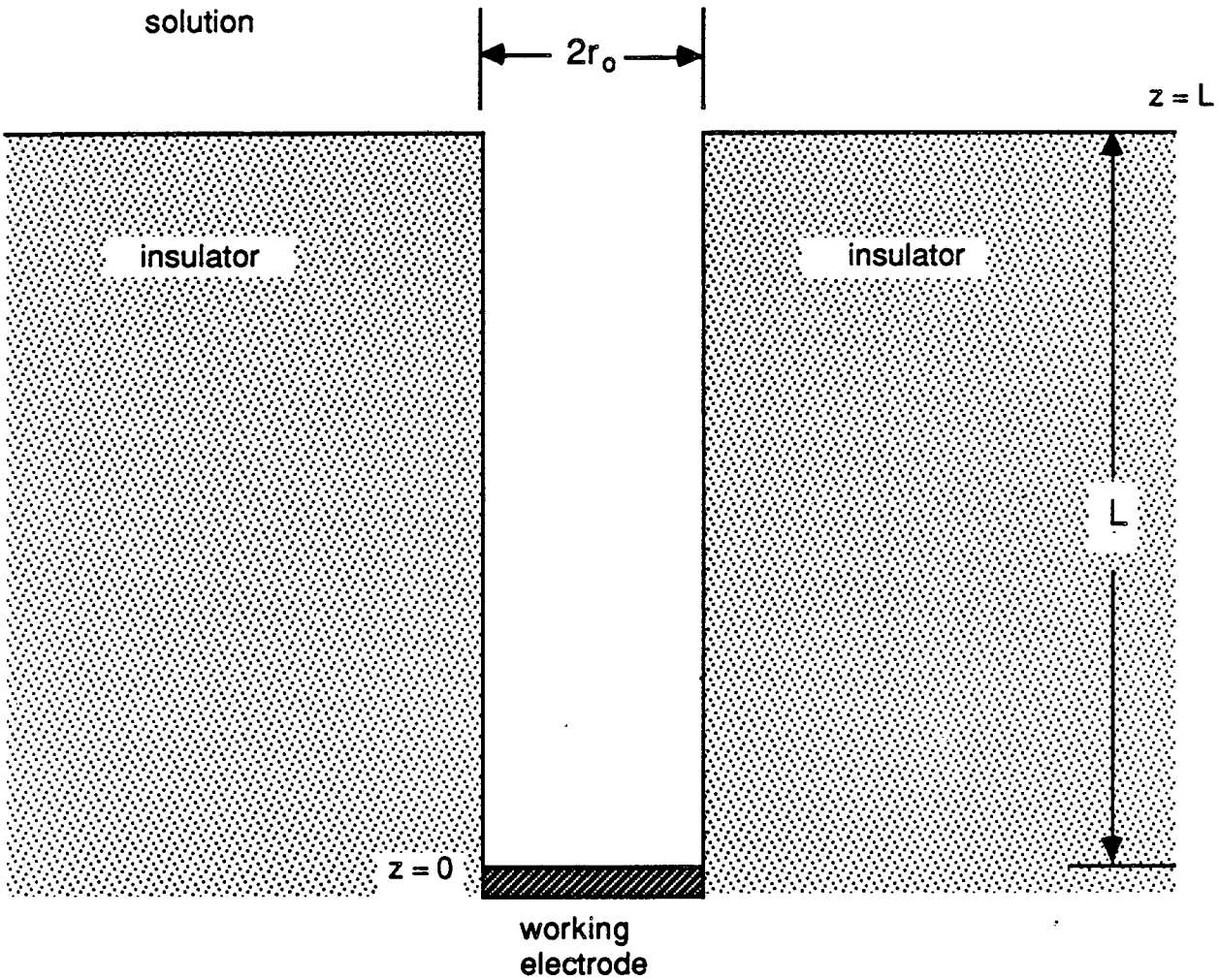

Figure 12. Schematic diagram of an axisymmetric, recessed disk electrode.

in the new geometry. As discussed in section 3.3, Laplace's equation maintains the same form. Therefore, equation (71) provides a simple numerical procedure to determine the potential from a known current distribution. After an explicit relation between the original and transformed coordinates is used, the governing integral equation can be written as

$$\Phi(x_q,y_q) = \Phi_* - \frac{1}{2\pi}\int_0^L \frac{i_{n,c}(x)}{\kappa} \ln\left[\sinh^2\left[\frac{\pi(x_q-x)}{2h}\right] + \sin^2\left[\frac{\pi(y_q-h)}{2h}\right]\right]dx - \frac{1}{2\pi}\int_0^L \frac{i_{n,a}(x)}{\kappa} \ln\left[\sinh^2\left[\frac{\pi(x_q-x)}{2h}\right] + \sin^2\left[\frac{\pi y_q}{2h}\right]\right]dx, \tag{87}$$

where Φ_* is a constant, which might be evaluated, for example, by requiring that the total currents on the two electrodes have the same magnitude but opposite sign:

$$0 = \int_0^L [\, i_{n,c}(x) + i_{n,a}(x) \,]dx. \tag{88}$$

If the current distribution is unknown but related to the local surface overpotential, an iterative procedure can determine the potential. Poddubnyi and Rudenko [99] used a similar method for linear kinetic distributions on a triangular-profiled cathode.

To describe how the current distribution deviates from a primary distribution, West and Newman [92] mapped the wedge shown in figure 1 so that the insulator and electrode are coplanar. The deviation ψ from the primary potential is given by

$$\psi_o(x_q) = \frac{\beta}{2\pi^2}\int_0^\infty \ln(x-x_q)^2 \left[f(\psi_o)x^{(\beta/\pi-1)} + x^{-1/2}\right]dx, \tag{89}$$

where $x = r^{\pi/\beta}$. In the original coordinate system, the normal gradient of the potential along the electrode is given by

$$\frac{1}{r}\frac{\partial \phi}{\partial \theta} = f(\psi_o), \tag{90}$$

and the quantity $x^{(\beta/\pi-1)}$ relates the derivative of potential in the original coordinate system to the derivative of potential in the new coordinate system. If the more specialized equation (89) is not used, ψ could be obtained from a procedure that requires finding simultaneously the potential on both the electrode and insulator; thus, the savings in computer costs can be substantial.

Instead of mapping geometries so that they are coplanar, two coordinate transformations could be used so that the electrodes are placed on opposite ends of a rectangle. An advantage to this procedure is that the conformal mapping effectively provides a proper mesh spacing in the original coordinate system, where an accurate solution may require the placement of more nodes near an electrode edge, where the current density varies rapidly.

4.3. Interpolation and Integration

To attain accurate solutions with the boundary integral equations discussed in sections 3.7 and 4.2, accurate integration and interpolation of the current density and potential are necessary. In particular, equations (80) and (81) are necessary to describe the behavior of singularities that arise in the determination of primary potential distributions. To help demonstrate how equations (80) and (81) are important, we discuss the evaluation of the boundary integral equations that describe the current distribution on a disk electrode.

If the primary current distribution, given by equation (82), were unknown, it could be determined from

$$i_n(r_q) = -\frac{2\kappa}{\pi}\int_{r_o}^{\infty}\frac{(\Phi(r)-\Phi_o)E(m)r}{(r-r_q)^2(r+r_q)}\,dr\,, \tag{91}$$

where equation (91) is obtained by differentiating equation (73) with respect to z_q. The primary potential distribution on the insulator [13],

$$\Phi^p(r) = \Phi_o^p\left[1-\frac{2}{\pi}\tan^{-1}(r^2/r_o^2-1)^{1/2}\right], \tag{92}$$

could be determined from equation (77). To evaluate these integral equations, the potential and current density would be approximated by interpolating between the points at which they are evaluated directly. Equation (80) shows that the current density near the electrode edge should be assumed to vary as $(r_o - r)^{-1/2}$. Interpolating the current density in this manner helps to eliminate numerical artifacts that often arise. Equation (81) suggests interpolating the potential along the insulator, near the electrode, as $(r - r_o)^{1/2}$.

As Edwards [100] discussed, an integrand with a singularity of the form x^{-n} as $x \longrightarrow 0$, can best be integrated by changing the variable of integration to Y, where $Y = x^{(1-n)/2}$ or $Y = x^{1-n}$. Equation (77) contains an integrable singularity of the form $(r_o-r)^{-1/2}$. This implies that it is advantageous to change the variable of integration to $Y = (r_o-r)^{1/2}$. After this change of variable, with the exact form of i_n substituted in, equation (77) becomes

$$\Phi(r_q) = \frac{2r_o i_{avg}}{\pi\kappa}\int_0^{\sqrt{r_o}}\frac{K(m)(r_o-Y^2)\,dY}{(2r_o-Y^2)^{1/2}(r_q+r_o-Y^2)}\,, \tag{93}$$

which eliminates the singularity caused by the current density as $r \longrightarrow r_o$. $K(m)$, though, still presents a problem because it contains a

logarithmic singularity when $r \longrightarrow r_q$. Logarithmic singularities can be handled by the method of Kantorovich and Krylov [101] or a special Gaussian quadrature formula [102].

For secondary current distributions, equation (91) is unnecessary because equation (77) and the relation between the surface overpotential and the current density are sufficient. For large, finite polarization parameters, the current distribution is highly nonuniform, although it is not singular. Such distributions, then, can be difficult to determine accurately, and the use of a function incorporating the asymptotic behavior discussed in section 3.8 should be helpful.

4.4. *Verifying Numerical Calculations*

Most numerical techniques are tested by solving problems that have been investigated by a more accurate procedure. The solutions of new problems are normally verified qualitatively by visually inspecting plots of potential or current distributions. For careful work, a more quantitative test of calculations might be desired. West *et al.* [24] discussed how previous singular perturbation analyses can be used to show when numerical methods fail as the polarization parameter becomes large. In their method, they concentrate on the current density at the edge of the electrode because, in this region, the distribution varies the most and, hence, is likely to be the most susceptible to errors.

Specifically, they suggested plotting i_{edge}/i_{avg} against $J^{(1 - \pi/2\beta)}$ for linear kinetics and against $\delta^{(2\beta/\pi - 1)}$ for Tafel kinetics, where J and δ are the appropriately defined polarization parameters for the geometry of interest. If the numerical calculations are accu-

rate, such plots vary linearly for large polarization parameters. Additionally, the slope that accurate calculations must follow can be predicted if P_o, as defined in section 4.1, is known. For linear kinetics, the slope is given by

$$\frac{i_{edge}}{P_o} = A_L(\beta)\left[\frac{(\alpha_a+\alpha_c)Fi_o}{RT\kappa}\right]^{(1-\pi/2\beta)}, \tag{94}$$

and, for Tafel kinetics,

$$\frac{i_{edge}}{P_o} = A_T(\beta)\left[\frac{\alpha_a FP_o}{RT\kappa}\right]^{(2\beta/\pi-1)}. \tag{95}$$

A_L and A_T are constants for a given angle of intersection between the electrode and insulator. They are shown in figure 13, which is reproduced from reference [24].

Since the primary current distribution is an important asymptotic distribution to determine, P_o will often be known. Therefore, a quantitative test of numerical procedures is available for many studies. It may also be important to develop tests for more general current distribution problems, where concentration variations play a role.

5. Conclusions

Techniques for solving Laplace's equation are reviewed. We emphasize that, even with the increasing availability of sophisticated computers, it is useful to know analytic and asymptotic solution methods. Our brief discussion indicates the more important methods and provides an overview of the literature, where more solution details and examples are given.

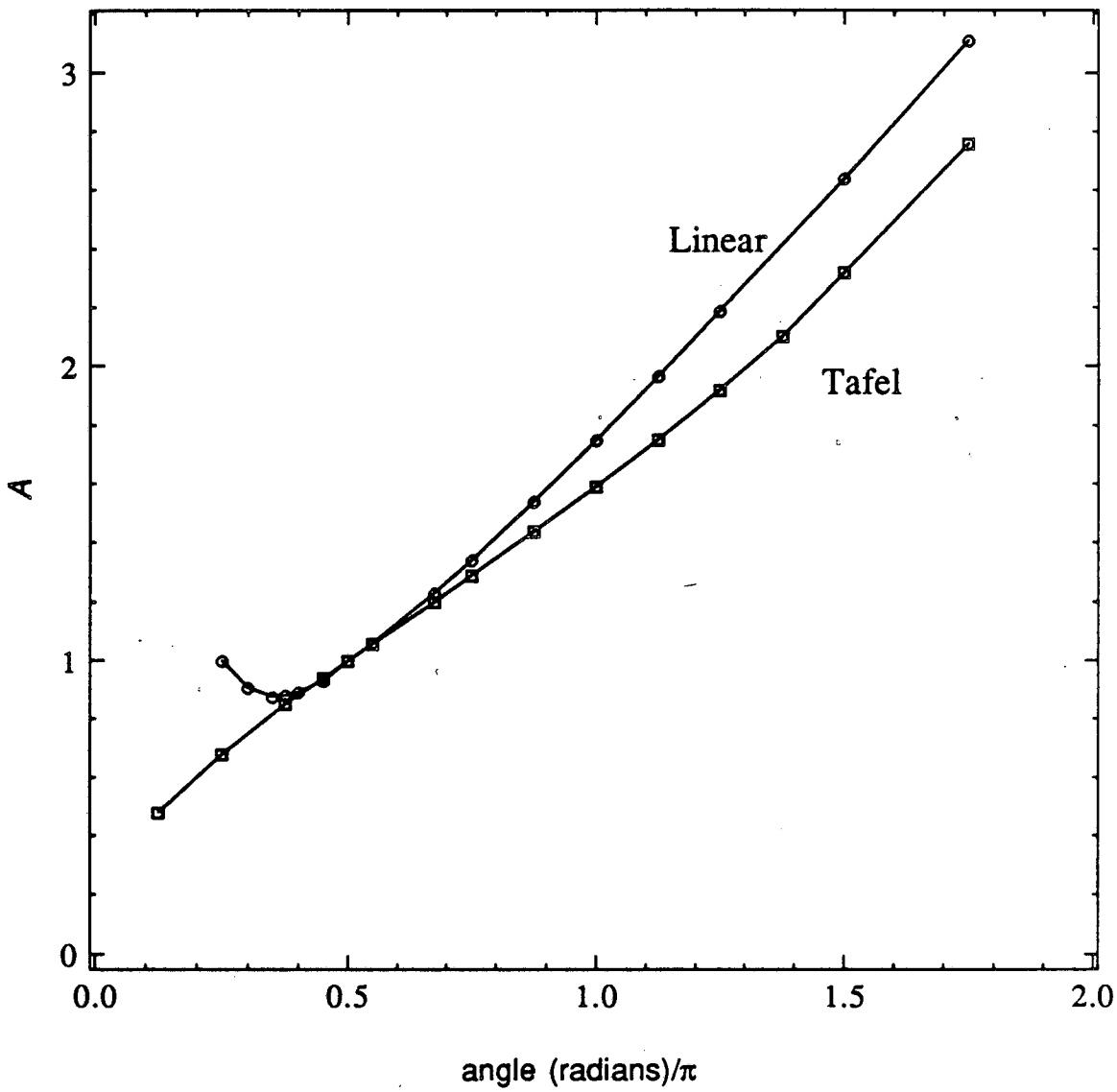

Figure 13. Dimensionless coefficient that can be used with equation (94) or (95) to determine the slope of the suggested plots for valid, numerical calculations for high polarization parameters and no concentration variations. (taken from reference [24]).

6. Acknowledgements

We would like to thank Vincent Battaglia, Thomas Fuller, Anthony Grabowski, and Paul Shain for helpful criticisms of this manuscript, and Kenneth G. Jordan for bringing to our attention some important papers.

This work was supported by the Assistant Secretary for Conservation and Renewable Energy, Office of Energy Storage and Distribution, Energy Storage Division, U. S. Department of Energy under Contract No. DE-AC03-76SF00098.

7. List of Symbols

a, C	constants used in the mappings shown in figure 5, cm
A_n, B_n, C_n	coefficients of a series
A_s, C_s	surface area and circumference shown in figure 9
C	double-layer capacity, F/cm
$\mathbf{e}_r, \mathbf{e}_z$	unit normal vectors
F	Faraday's constant, 96487 C/equiv
g	Green's function, cm^{-1}
h_n	normal distance to the boundary, cm
i	current density, A/cm^2
i_n	normal component of the current density, A/cm^2
i_o	exchange current density, A/cm^2
j	$\sqrt{-1}$
J	dimensionless exchange current density

J_n	Bessel function of the first kind of order n
$K(m), E(m)$	complete elliptic integral of the first and second kinds
L, W	characteristic lengths, cm
m, n	characteristic lengths of a recessed electrode, cm
M	molecular weight, g/mol
P_o	parameter defined in equation (80), A/cm$^{(1+\pi/2\beta)}$
P_{2n}	even Legendre polynomials
R	universal gas constant, 8.3143 J/mol-K
r, z, θ	cylindrical coordinates, cm
r_o	radius of the disk or the mercury drop, cm
t	time, s
T	absolute temperature, K
V	electrode potential, V
Wa	Wagner number
$W\kappa R$	dimensionless cell resistance of a recessed electrode
x, y, z	Cartesian coordinates, cm
α_a, α_c	transfer coefficients
α_2, α_3	coefficients defined in figure 9
β	angle shown in figure 1, radians
$\delta(x_q, y_q, z_q)$	Dirac delta function
δ	dimensionless average current density
η, ξ	rotational elliptic coordinates
η	similarity variable used in section (3.5)
κ	solution conductivity, S/cm
λ_n	n^{th} root of $J_1(x)$

η_s	surface overpotential, V
μ,ν	tangent-sphere coordinates
ξ_2	distance for two-dimensional geometries, cm
ξ_3	distance for three-dimensional geometries, cm
π	3.141592654
ρ	deposit density, g/cm^3
τ	time constant, s
Φ	potential of the solution, V
Φ_o	solution potential adjacent to the electrode, V
Ψ	potential defined by equation (41)
ψ_n	orthogonal polynomials
ω	frequency, s^{-1}

Subscripts

avg	average
i,r	imaginary and real parts of a complex variable
max	maximum
q	coordinate at which the potential is being solved
ss	steady state

8. References

[1] John Newman, "Current Distribution on a Rotating Disk below the Limiting Current," *J. Electrochem. Soc.*, 113, 1235 (1966).

[2] John S. Newman, *Electrochemical Systems*, Prentice-Hall, Englewood Cliffs, N. J. (1973).

[3] W. R. Parrish and John Newman, "Current Distributions on Plane, Parallel Electrodes in Channel Flow," *J. Electrochem. Soc.*, 117, 43 (1970).

[4] Victoria Edwards and John Newman, "Design of Thin-Gap Channel Flow Cells," *J. Electrochem. Soc.*, 134, 1181 (1987).

[5] Peter Pierini and John Newman, "Current Distribution on a Rotating Ring-Disk Electrode below the Limiting Current," *J. Electrochem. Soc.*, 124, 701 (1977).

[6] Richard Alkire and Ali Asghar Mirarefi, "The Current Distribution Within Tubular Electrodes under Laminar Flow," *J. Electrochem. Soc.*, 120, 1507 (1973).

[7] Geoffrey A. Prentice and Charles W. Tobias, "A Survey of Numerical Methods and Solutions for Current Distribution Problems," *J. Electrochem. Soc.*, 129, 72 (1982).

[8] N. Ibl, "Current Distribution," *Comprehensive Treatise of Electrochemistry*, 6, Ernest Yeager, J. O'M. Bockris, Brian E. Conway, S. Sarangapani, Editors, p. 239, Plenum Press, New York (1983).

[9] John Newman, "The Fundamental Principles of Current Distribution and Mass Transport in Electrochemical Cells," in *Electroanalytical Chemistry*, A. J. Bard, Editor, p. 187, Marcel-Dekker, Inc., New York (1973).

[10] R. N. Fleck, *Numerical Evaluation of Current Distribution in Electrochemical Systems*, M. S. Thesis, University of California, Berke-

ley (1964).

[11] Kaoru Kojima, "Engineering Analysis of Electrolytic Cells: Electric Resistance between Electrodes," *Res. Rep. F. Engg. Niigata Univ.*, 13, 183 (1964).

[12] H. S. Carslaw and J. C. Jaeger, *Conduction of Heat in Solids*, Clarendon Press, Oxford (1959).

[13] John Newman, "Resistance for Flow of Current to a Disk," *J. Electrochem. Soc.*, 113, 501 (1966).

[14] Joseph J. Miksis Jr. and John Newman, "Primary Resistances for Ring-Disk Electrodes," *J. Electrochem. Soc.*, 123, 1030 (1976).

[15] Peter Pierini and John Newman, "Potential Distribution for Disk Electrodes in Axisymmetric Cells," *J. Electrochem. Soc.*, 126, 1348 (1979).

[16] Ralph White and John Newman, "Simultaneous Reactions on a Rotating-Disk Electrode," *J. Electroanal. Chem.*, 82, 173 (1977).

[17] Leonard Nanis and Wallace Kesselman, "Engineering Applications of Current and Potential Distributions in Disk Electrode Systems," *J. Electrochem. Soc.*, 118, 454 (1971).

[18] John Newman, D. N. Hanson, and K. Vetter, "Potential Distribution in a Corroding Pit," *Electrochimica Acta*, 122, 829 (1977).

[19] Der-Tau Chin, "Convective-Diffusion on a Rotating Spherical Electrode," *J. Electrochem. Soc.*, 118, 1434 (1972).

[20] Kemal Nisancioglu and John Newman, "Current Distribution on a Rotating Sphere below the Limiting Current," *J. Electrochem. Soc.*, 121, 241 (1974).

[21] John Newman, "Mass Transport and Potential Distribution in the Geometries of Localized Corrosion," presented at *International Conference of Localized Corrosion*, Orlando, FL (June 1, 1987).

[22] John Newman, "Mass Transport and Potential Distribution in the Geometries of Localized Corrosion," in *Localized Corrosion*, B. F. Brown, J. Kruger, and R. W. Staehle, Editors, p. 45, National Association of Corrosion Engineers, Houston (1974).

[23] Carl Wagner, "Theoretical Analysis of the Current Density Distribution in Electrolytic Cells," *J. Electrochem. Soc.*, **98**, 116 (1951).

[24] Alan C. West, Johannes H. Sukamto, and John Newman, "A Criterion to Verify Current Distribution Calculations," *J. Electrochem. Soc.*, submitted.

[25] Charles Kasper, "The Theory of the Potential and the Technical Practice of Electrodeposition. III. Linear Polarization on Some Line-Plane Systems," *Trans. Electrochem. Soc.*, **78**, 131 (1940).

[26] T. P. Hoar and J. N. Agar, "Factors in Throwing Power Illustrated by Potential-Current Diagrams," *Discussions of the Faraday Soc.*, 1, 162 (1947).

[27] John Newman, "Engineering Design of Electrochemical Systems," *Ind. Eng. Chem.*, **60**, 12 (1968).

[28] Alan C. West and John Newman, "Interpretation of Kinetic Rate Data Taken in a Channel Flow Cell," *J. Electrochem. Soc.*, 136, 3755 (1989).

[29] Philip Paul Russell, *Corrosion of Iron: The Active-Passive Transition and Sustained Electrochemical Oscillations*, Ph. D. Thesis, University of California, Berkeley (1984).

[30] Marcel Porbaix, *Atlas of Electrochemical Equilibria in Aqueous Solutions*, p. 315, National Association of Corrosion Engineers, Houston (1974).

[31] Clarence G. Law, Jr. and John Newman, "A Model for the Anodic Dissolution of Iron in Sulfuric Acid," *J. Electrochem. Soc.*, 126, 2150 (1979).

[32] Philip Russell and John Newman, "Anodic Dissolution of Iron in Acidic Sulfate Electrolytes, II. Mathematical Model of Current Oscillations Observed under Potentiostatic Conditions," *J. Electrochem. Soc.*, 134, 1051 (1987).

[33] Chrystalla C. Haili, *The Corrosion of Iron Rotating Hemispheres in 1 M Sulfuric Acid: An Electrochemical Impedance Study*, M. S. Thesis, University of California, Berkeley (1987).

[34] John Owen Dukovic, *Studies on Current Distribution in Electrochemical Cells*, Ph. D. Thesis, University of California, Berkeley (1986).

[35] Kemal Nişancioğlu and John Newman, "The Transient Response of a Disk Electrode," *J. Electrochem. Soc.*, 120, 1339 (1973).

[36] Kemal Nişancioğlu and John Newman, "The Transient Response of a Disk Electrode with Controlled Potential," *J. Electrochem. Soc.*, 120, 1346 (1973).

[37] Kemal Nişancioğlu and John Newman, "The Short-Time Response of a Disk Electrode," *J. Electrochem. Soc.*, 121, 523 (1974).

[38] John Newman, "Ohmic Potential Measured by Interrupter Techniques," *J. Electrochem. Soc.*, 117, 507 (1970).

[39] John Newman, "Frequency Dispersion in Capacity Measurements at a Disk Electrode," *J. Electrochem. Soc.*, 117, 198 (1970).

[40] Carl Wagner, "Contribution to the Theory of Electropolishing," *J. Electrochem. Soc.*, 101, 225 (1954).

[41] Peter Fedkiw, "Primary Current Distribution on a Sinusoidal Profile," *J. Electrochem. Soc.*, 127, 1304 (1980).

[42] Richard Alkire, Terry Bergh, and Robert L. Sani, "Predicting Electrode Shape Change with Use of Finite Element Methods," *J. Electrochem. Soc.*, 125, 1981 (1978).

[43] J. B. Riggs, R. H. Muller, and C. W. Tobias, "Prediction of Work Piece Geometry in Electrochemical Cavity Sinking," *Electrochim. Acta*, 26, 961 (1981).

[44] G. A. Prentice and C. W. Tobias, "Simulation of Changing Electrode Profiles," *J. Electrochem. Soc.*, 129, 78 (1982).

[45] J. Deconinck, G. Maggetto, and J. Vereecken, "Calculation of Current Distribution and Electrode Shape Change by the Boundary Element Method," *J. Electrochem. Soc.*, 132, 2960 (1985).

[46] Edward C. Hume, III, William M. Deen, and Robert A. Brown, "Mass Transfer Analysis of Electrodeposition Through Polymeric Masks," *J. Electrochem. Soc.*, 131, 1251 (1984).

[47] Uziel Landau, in "Zinc Electrodeposition and Dendritic Growth from Zinc Halide Electrolytes," EPRI Report EM-2393, Electric Power Research Institute, Palo Alto, CA (1982).

[48] Dale P. Barkey, Rolf H. Muller, and Charles W. Tobias, "Roughness Development in Metal Deposition. II. Stability Theory," *J. Electrochem. Soc.*, 136, 2207 (1989).

[49] Dale Paul Barkey, *Studies on High Speed Electroforming*, Ph. D. Thesis, University of California, Berkeley (1987).

[50] Ryoichi Aogaki and Tohru Makino, "Theory of Powdered Metal Formation in Electrochemistry—Morphological Instability in Galvanostatic Crystal Growth under Diffusion Control," *Electrochimica Acta*, 26, 1509 (1981).

[51] W. W. Mullins and R. F. Sekerka, "Stability of a Planar Interface During Solidification of a Dilute Binary Alloy," *J. App. Phys.*, 35, 444 (1964).

[52] Frank M. White, *Viscous Fluid Flow*, chapter 5, McGraw-Hill, New York (1974).

[53] J. A. Klingert, S. Lynn, and C. W. Tobias, "Evaluation of Current Distribution in Electrode Systems by High-Speed Digital Computers," *Electrochim. Acta*, 9, 297 (1964).

[54] Leon Lapidus and George F. Pinder, *Numerical Solution of Partial Differential Equations in Science and* Engineering, John Wiley & Sons, New York (1982).

[55] C. A. J. Fletcher, *Computational Galerkin Methods*, Springer-Verlag, New York (1984).

[56] J. A. Liggett and P. L-F. Liu, *The Boundary Integral Equation Method for Porous Media Flow*, Allen and Unwin, Boston (1983).

[57] C. A. Brebbia, *The Boundary Element Methods for Engineers*, John Wiley and Sons, New York (1981).

[58] P. K. Banerjee and R. Butterfeld, *Boundary Element Methods for Engineering Science*, McGraw-Hill Inc., New York (1981).

[59] E. C. Hume III, R. A. Brown, and W. M. Deen, "Comparison of Boundary and Finite Elements Methods for Moving-Boundary Problems Governed by a Potential," *Int. J. Num. Meth. Eng.*, 21, 1295 (1985).

[60] M. Matlosz, C. Creton, C. Clerc, and D. Landolt, "Secondary Current Distribution in a Hull Cell. Boundary Element and Finite Element Simulation and Experimental Verification," *J. Electrochem. Soc.*, 134, 3015 (1987).

[61] B. D. Cahan, Daniel Scherson, Margaret A. Reid, "I-BIEM. An Iterative Boundary Integral Equation Method for Computer Solutions of Current Distribution Problems with Complex Boundaries—A New Algorithm," *J. Electrochem. Soc.*, 135, 285 (1988).

[62] Peter Pierini and John Newman, "Ring Electrodes," *J. Electrochem. Soc.*, 125, 79 (1978).

[63] Rael Morris and William Smyrl, "Galvanic Interactions on Periodically Regular Heterogeneous Surfaces," *AIChE Journal*, 34, 723 (1988).

[64] Rael Morris and William Smyrl, "Galvanic Interactions on Random Heterogeneous Surfaces," *J. Electrochem. Soc.*, 136, 3237 (1989).

[65] H. Shih and H. W. Pickering, "Three-Dimensional Modeling of the Potential and Current Distributions in an Electrolytic Cell," *J. Electrochem. Soc.*, 134, 551 (1987).

[66] N. G. Zamani, J. F. Porter, and A. A. Mufti, "A Survey of Computational Efforts in the Field of Corrosion Engineering," *Int. J. Numer. Methods Eng.*, 23, 1295 (1986).

[67] Mark E. Orazem and John Newman, "Primary Current Distribution of a Slotted-Electrode Cell," *J. Electrochem. Soc.*, 131, 2857 (1984).

[68] Conrad B. Diem, Bernard Newman, and Mark E. Orazem, "The Influence of Small Machining Errors on the Primary Current Distribution at a Recessed Electrode," *J. Electrochem. Soc.*, 135, 2524 (1988).

[69] Paul J. Sides and Charles W. Tobias, "Primary Potential and Current Distribution Around a Bubble on an Electrode," *J. Electrochem. Soc.*, 127, 288 (1980).

[70] Parry Moon and Domina E. Spencer, *Field Theory Handbook*, Spring-Verlag, Berlin (1961).

[71] H. Fletcher Moulton, "Current Flow in Rectangular Conductors," *Proceedings of the London Mathematical Society*, (ser. 2), 3, 104 (1905).

[72] R. V. Churchill, *Complex Variables and Applications*, 2nd Edition, McGraw-Hill, New York (1960).

[73] M. Abramowitz and I. A. Stegun, Editors, *Handbook of Mathematical Functions*, National Bureau of Standards, Washington (1964).

[74] Alan C. West and John Newman, "Current Distributions on Recessed Electrodes," *J. Electrochem. Soc.*, submitted.

[75] Francis B. Hildebrand, *Advanced Calculus for Applications*, Prentice-Hall, Inc., Englewood Cliffs, N. J. (1976).

[76] John Newman and J. E. Harrar, "Potential Distribution in Axisymmetric Mercury-Pool Electrolysis Cells at the Limiting Current," *J. Electrochem. Soc.*, 120, 1041 (1973).

[77] Francis B. Hildebrand, *loc. cit.*, p. 203.

[78] L. I. Sedov, *Similarity and Dimensional Methods in Mechanics*, Academic Press, New York (1959).

[79] Hermann Schlichting, *Boundary-Layer Theory*, 7th Edition, McGraw-Hill, New York (1979).

[80] Milan M. Jakšić and John Newman, "The Kramers-Kronig Relations and Evaluation of Impedance for a Disk Electrode," *J. Electrochem. Soc.*, 133, 1097 (1986).

[81] S. H. Glarum, "Variation Approximations to Current Distribution Problems. The Rotating Disk Electrode," *J. Electrochem. Soc.*, 124, 518 (1977).

[82] S. H. Glarum and J. H. Marshall, "An AC Admittance Study of the Platinum/Sulfuric Acid Interface," *J. Electrochem. Soc.*, 126, 424 (1979).

[83] W. H. Mulder and J. H. Sluyters, "An Explanation of Depressed Semi-Circular Arcs in Impedance Plots for Irreversible Electrode Reactions," *Electrochimica Acta*, 33, 303 (1988).

[84] A. Le Mehaute and G. Crepy, "Introduction to Transfer and Motion in Fractal Media: The Geometry of Kinetics," *Solid State Ionics*, 9 and 10, 17 (1983).

[85] Thomas C. Halsey, "Frequency Dependence of the Double-Layer Impedance at a Rough Surface," *Phys. Rev. A*, 35, 3512 (1987).

[86] Bernard Tribollet and John Newman, "Impedance Model for a Concentrated Solution. Application to the Electrodissolution of Copper in Chloride Solutions," *J. Electrochem. Soc.*, 131, 2780 (1984).

[87] Bernard Tribollet and John Newman, "The Modulated Flow at a Rotating Disk Electrode," *J. Electrochem. Soc.*, 130, 2016 (1983).

[88] John David Jackson, *Classical Electrodynamics*, 2nd edition, John Wiley & Sons, New York (1975).

[89] Michael D. Greenberg, *Applications of Green's Functions in Science and Engineering*, Prentice-Hall, Englewood Cliffs, N. J. (1971).

[90] L. C. Wrobel and C. A. Brebbia, "Axisymmetric Potential Problems," *New Developments in Boundary Element Methods, Proceedings of the Second International Seminar*, Southampton, pp. 77-89 (1980).

[91] William H. Smyrl and John Newman, "Current Distribution at Electrode Edges at High Current Densities," *J. Electrochem. Soc.*, 136, 132 (1989).

[92] Alan C. West and John Newman, "Current Distribution Near an Electrode Edge as a Primary Distribution is Approached," *J. Electrochem. Soc.*, 136, 2935 (1989).

[93] Milton Van Dyke, *Perturbation Methods in Fluid Mechanics*, The Parabolic Press, Stanford, California, Annotated Edition (1975).

[94] J. R. Bowen, A. Acrivos, and A. K. Oppenheim, "Singular Perturbation Refinement to Quasi-Steady State Approximation in Chemical Kinetics," *Chem. Eng. Sci.*, 18, 177 (1963).

[95] Ian Proudman and J. R. A. Pearson, "Expansions at Small Reynolds Numbers for the Flow Past a Sphere and a Circular Cylinder," *J. Fluid Mech.*, 2, 387 (1962).

[96] Reinaldo Cabán and Thomas W. Chapman, "Rapid Computation of Current Distribution by Orthogonal Collocation," *J. Electrochem. Soc.*, 123, 1036 (1976).

[97] John Villadsen and Michael L. Michelsen, *Solution of Differential Equation Models by Polynomial Approximations*, Prentice-Hall, Englewood Cliffs, N. J. (1978).

[98] Francis B. Hildebrand, *loc. cit.*, p. 149.

[99] N. P. Poddubnyi and E. I. Rudenko, "Conformal Mapping in Calculation of Secondary Current Distribution in Electrolytic Cells," *Elekrokhimiya*, 8, 943 (1968).

[100] Victoria Edwards, *Design of Thin-Gap Channel Flow Cells*, Ph. D. Thesis, University of California, Berkeley (1986).

[101] L. V. Kantorovich and V. J. Krylov, *Approximate Methods of Higher Analysis*, translated by C. D. Benter, Interscience Publishers, New York (1959).

[102] A. H. Stroud and Don Secrest, *Gaussian Quadrature Formulas*, Prentice-Hall, Englewood Cliffs, N. J. (1966).

LAWRENCE BERKELEY LABORATORY
TECHNICAL INFORMATION DEPARTMENT
1 CYCLOTRON ROAD
BERKELEY, CALIFORNIA 94720